ASSESSING THE MECHANICAL AND MICROSTRUCTURAL PROPERTIES OF CONCRETE WITH ELECTRIC ARC FURNACE SLAG REPLACEMENT AT 60%, 75% AND 90%

CHANG SHAO HERN

UNIVERSITI TUNKU ABDUL RAHMAN

ASSESSING THE MECHANICAL AND MICROSTRUCTURAL PROPERTIES OF CONCRETE WITH ELECTRIC ARC FURNACE SLAG REPLACEMENT AT 60%, 75% AND 90%

CHANG SHAO HERN

A project report submitted in partial fulfilment of the requirements for the award of Bachelor of Civil Engineering with Honours

Lee Kong Chian Faculty of Engineering and Science
Universiti Tunku Abdul Rahman

May 2025

DECLARATION

I hereby declare that this project report is based on my original work except for citations and quotations which have been duly acknowledged. I also declare that it has not been previously and concurrently submitted for any other degree or award at UTAR or other institutions.

Name : Chang Shao Hern

ID No. : 21UEB02021

Date : 28/5/2025

COPYRIGHT STATEMENT

This final year project report is submitted in partial fulfilment of the requirements for the degree of Bachelor of Civil Engineering with Honours at Universiti Tunku Abdul Rahman (UTAR). This final year project report represents the work of the author, except where due acknowledgement has been made in the text. No part of this final year project report may be reproduced, stored, or transmitted in any form or by any means, whether electronic, mechanical, photocopying, recording, or otherwise, without the prior written permission of the author or UTAR, in accordance with UTAR's Intellectual Property Policy.

ACKNOWLEDGEMENTS

I would like to thank everyone who had contributed to the successful completion of this project. I would like to express my deepest gratitude to my research supervisor, Ir. Ts. Dr. Lee Foo Wei for his invaluable advice, guidance and his enormous patience throughout the development of the research.

In addition, I would also like to express my gratitude to Mr. Jason Ting Jing Cheng and the lab officer who helped me and provided guidance for the lab work throughout the research study. Besides, I would like to thank my research partner Mr Harry Kueh Wei Kang for his assistance in the research study. Finally, I would like to thank all those who have assisted me indirectly during the report writing and lab session.

ABSTRACT

Nowadays, reusing the industrial by-products by aiming on sustainable objectives has risen as a important move in reducing the environmental impact by construction field. The objective of this study is to determine the mechanical properties which is compressive strength through evaluating the microstructural properties of elemental and chemical compound composition of concrete with EAF slag replacement for natural fine aggregates at different ratios of 60%, 75% and 90% for acrossing three particle size ranges (R1: 0.8 to 2.36 mm, R2: 2.36 to 4.75 mm and R3: 4.75 to 6.30 mm). Optimal replacement ratio which could provide optimum replacement ratio is also being determined. A total of 30 concrete samples were prepared and tested by using 5 tests which including of Compressive Strength Test, Scanning Electron Microscopy (SEM) Test, Energy Dispersive X-ray Spectroscopy (EDX) Test, X-ray Diffraction (XRD) Test and Thermogravimetric Analysis (TGA) Test. The Compressive Strength Test shows that all EAF slag mixes concrete samples outperformed the control sample with the highest strength of 54.75 MPa. SEM Test had showed visibility of hydration products such as Ettringite, Portlandite and C-S-H gel in the microstructural of concrete samples casted. EDX Test indicated existence of several elements but Calcium and Silicon as the elemental composition which contributes to affect the compressive strength. Results of XRD Test validated the presence of compounds such as $Ca(OH)_2$, $CaCO_3$, SiO_2 and CaO and suggest that $Ca(OH)_2$ and $CaCO_3$ could contribute to affect the compressive strength. TGA Test presented the thermal stability of EAF slag replaced concrete for up to approximately 660°C before degradation starts. Overall, the results shows that a 90% replacement of fine aggregate with EAF slag using the R1 particle size range (0.8–2.36 mm) achieved the highest compressive strength of 54.75 MPa. Supported by favorable elemental (Ca and Si) and compound-level ($Ca(OH)_2$ and SiO_2) microstructural characteristics, this mix was identified as the optimal replacement ratio in this study. These findings could provide insights for the potential of EAF slag as a sustainable and performing alternative to natural fine aggregates. This also alignes with environmental and structural demands in modern construction practices.

Keywords: Electric Arc Furnace (EAF) Slag, Concrete, Fine Aggregate Replacement, Compressive Strength, Microstructure

Subject Area: TH1000-1725 Systems of building construction Including fireproof construction, concrete construction

TABLE OF CONTENTS

LIST OF TABLES

LIST OF FIGURES

LIST OF SYMBOLS / ABBREVIATIONS

Al	Aluminum
BSE	Backscattered Electrons
BOF	Basic Oxygen Furnace
C	Carbon
Ca	Calcium
$CaCO_3$	Calcium Carbonate
CaO	Calcium Oxide
$Ca(OH)_2$	Calcium Hydroxide
$CaSO_4.2H_2O$	Calcium Sulfate Hydrate
CCS	Carbon Capture and Storage
CCU	Carbon Capture and Utilization
CO_2	Carbon Dioxide
EAF	Electric Arc Furnace
EDX	Energy-Dispersive X-Ray Spectroscopy
LF	Ladle Furnace
Mg	Magnesium
MgO	Magnesium Oxide
O	Oxygen
OPC	Ordinary Portland Cement
SEM	Scanning Electron Microscopy
Si	Silica
SiO_2	Silicon Dioxide
TGA	Thermogravimetric Analysis
XRD	X-Ray Diffraction

CHAPTER 1

INTRODUCTION

1.1 General Introduction

In the current era, environmental sustainability and effective resource management have become major concerns among the public and governmental organizations worldwide. In particular, the construction industry is often being urged to reduce the environmental impact by minimizing waste generation and conserving natural resources. Concrete which is one of the most widely used construction material usually demands large quantities of natural aggregates. However, the extraction of these natural aggregates leads to environmental degradation. Therefore, alternative materials that can partially or fully replace natural aggregates without too much impact on performance are being studied to further determine this possibility.

One of the material being studied is Electric Arc Furnace (EAF) slag. This is a by-product produced during steel manufacturing. Generally, steel production generates a significant quantity of by-products with approximately 0.12 to 0.20 tonnes of slag produced per tonne of metal (Ragipani, Bhattacharya and Suresh, 2021). If this condition is not properly managed, slags can causes environmental risks due to the leaching of heavy metals and the long-term occupation of landfill space. Therefore, reusing EAF slag as a replacement material in concrete had been proposed as a sustainable solution to reduce environmental impacts while can still contributing to the circular economy in the construction sector.

Next, the utilization of EAF slag also complies with global efforts to reduce indirect carbon dioxide (CO_2) emissions which usually comes with traditional concrete production. Although CO_2 emissions are usually produced by combustion of fossil fuels, significant amounts are also due to the extraction, processing and transportation of raw aggregates. By incorporating industrial by-products such as EAF slag into concrete mixtures, the demand for natural aggregate mining is reduced and this also indirectly reducing CO_2 emissions from the construction supply chain (Shi, 2004).

Other than environmental benefits, EAF slag also provides favourable mechanical and chemical properties for concrete applications. The properties such as high density, angular shape and mineralogical composition which are rich in calcium silicates and iron oxides could further enhance the mechanical strength and durability of concrete when being incorporated in an appropriate quantity (Rondi *et al.*, 2016). However, the influence of replacement ratios and the microstructural characteristics of slag on concrete performance must be prior tested to ensure optimal performance.

Therefore, this research aims to assess the mechanical and microstructural properties of concrete by replacing natural fine aggregates with EAF slag at 60%, 75% and 90% replacement ratios. By evaluating the parameters such as compressive strength, hydration products and microstructural development, this study hopes to promote more sustainable practices in construction while still optimizing performance.

1.2 Importance of the Study

To further optimize the effect of partially replacing the EAF slag into concrete as fine aggregate, this study is vital to provide some insights on this topic. This study assess the mechanical and microstructural performance of concrete when natural fine aggregates are partially replaced by EAF slag at varying replacement ratios which are 60%, 75% and 90%. Identifying the optimal replacement ratios which could provide the optimal compressive strength is vital as this can contributes to a compressive strength which is optimal, better resistance to mechanical wear and enhanced durability against aggressive environmental conditions (Shi, 2004). This is especially valuable for construction applications requiring durable and high-strength materials as this optimal replacement ratio can let the concrete used have optimal performance.

Utilization of EAF slag in concrete brings many environmental benefits. By partially replacing natural fine aggregates such as sand with EAF slag, this helps to conserve natural resources by reducing the quarrying activities which causes ecological disruption. The incorporation of these industrial by-products into construction materials also gives opportunity to reduce the indirect carbon footprint of the industry. This can be done due to reducing the demand for raw material extraction and the emissions from mining and transportation

processes which cause by the extraction activities. Effective utilization of EAF slag also improve waste management issues by minimizing the environmental risks due to disposal of slag which may cause soil and groundwater contamination.

The study determines the microstructural properties of concrete which more specifically the elemental composition through EDX test and chemical compound identification through XRD test to understand how these factors influence development of optimal compressive strength. These insights can provide a guidance for future material design by linking microstructure to mechanical performance and making this research beneficial for both academic study and practical application.

1.3 Problem Statement

Construction industry from all over the world had contributed to the growth of economy since a long time ago. It had been an important catalyst for the economy growth. This causes the demand for construction materials to be increasing also to provide sufficient supply to the growth of construction industry. These materials are such as cement and aggregates which are the most common used in the construction industry. However, the nature resource could be depleted under this demand. Alternative materials are required to further address this issue. Steel manufacturing had also been growing since a long time ago where these 2 industries have close relationships and contributions for the economy growth. Slag which is a by-product produced during the steel manufacturing process had always been an issue for its disposing part. The conventional method which had been used all the time are incineration and landfilling could cause harmful environmental issues. There had been some ideas of utilizing these slags in the construction materials as this could conserve the environment but also covers the demand for construction at the same time. However, this brings out the issue of how is the effect of slags when being used to replace part of the materials which forms the concrete. Mechanical properties is an important part of concrete as this defines the amount of load or strength which can be handled. Therefore, it is crucial to study about how is the impact on mechanical properties after part of it had been replaced with slags produced from steel manufacturing.

Most existing studies involving EAF slag as a partial replacement for fine aggregate have concentrated on low to moderate replacement levels which is typically until 50% to 75% where mechanical performance tends to remain or improve based on (Pellegrino & Gaddo, 2009) and (Manso *et al*., 2004). However, there is limited research on the effects of high-volume replacements which particularly above 60% although it has potential to significantly reduce natural resource consumption and promote more sustainable waste utilization. Some published findings shows that excessively high slag content may causes reductions in compressive strength or long-term durability but conclusive data remains scarce. To mitigate this situation, the present study focuses on replacement ratios of 60%, 75% and 90% which fall within the moderate to high range. These levels are selected to evaluate how increasing slag content affects compressive strength. The findings would like to determine whether high slag content imposes changes in strength development.

It is also worth to consider that one of the physical characteristics of the slag which is particle size may influence performance outcomes. As noted in ASTM C33, the 4.75 mm sieve is a value to differenciate fine and coarse aggregates which could makes it a reference point. In this context, the range of particle sizes selected in this study which contain below, around and above this point provides opportunity to observe how variations in slag sizes may contribute to differences in strength development. These observations may offer additional insights into optimizing the material's use in concrete applications.

1.4 Aim and Objectives

This study aims to determine the mechanical properties which is compressive strength through evaluating the microstructural properties of elemental and chemical compound composition of concrete with EAF slag replacement as fine aggregate. The specific objectives of the study are as follows:

(i) To compare the compressive strength between EAF slag concrete and conventional concrete.

(ii) To determine the optimal replacement ratio of EAF slag which could provide optimal compressive strength.

(iii) To study the elemental and chemical compound composition which affect the compressive strength of concrete with EAF slag replacing fine aggregate at ratio of 60%, 75% and 90%.

In addition to evaluating performance, this study also supports sustainable construction practices by exploring the potential of EAF slag which is a steel industry by-product as a partial replacement for natural fine aggregates. Utilizing EAF slag helps reduce dependent on natural sand resources and minimizes environmental impact by promoting industrial waste reuse and reducing the ecological footprint of concrete production.

1.5 Scope and Limitation of the Study

Through the determination of these mechanical and microstructural properties, this study attempts to explore the technical features of steel slags which offering insights into their performance and behavior for useful applications. Instead of using BOF or LF steel slag, the slag used in this study is called EAF slag. The particle used for this study is being categorized into 3 categories which are 0.8mm to 2.36mm, 2.36mm to 4.75mm and 4.75mm to 6.3mm. These sizes also aligns with the sizes of sieves available in the laboratory. The steel slag is oven-dried in oven.

The replacement ratio of EAF slags as fine aggregate in the concrete sample which being studied in this case are 60%, 75% and 90%. A total of 30 samples were prepared for this study. Atomic weight percentages can be easily determined by using Energy Dispersive X-ray (EDX) testing to examine the elemental composition of the EAF slag. Chemical compounds which are available could be determined with the aid of X-ray Diffraction (XRD). Using scanning electron microscopy (SEM), the surface morphologies of the EAF slag sample are examined. Compressive Strength Test is also carried out to determine the compressive strength of sample which is the mechanical properties studied. Thermal stability of the samples could be determined by Thermogravimetric Analysis (TGA).

There are some constraints limiting this study that could affect its accuracy and development. First, the EAF slag samples used in this study originated from one source only which is from Penang, Malaysia. This study

ignores other sources of EAF slag due to limited sources and this could cause inaccuracy of data obtained as this study does not have enough data to compare. However, this study acknowledges the availability of other sources in Malaysia and worldwide. This study only focus on the compressive strength for the mechanical properties as this strength is the most important for concrete. One of the main characteristics of concrete is could withstand large amount of compressive load applied.

1.6 Contribution of the Study

This study contributes to the promoting of sustainable construction practices by using Electric Arc Furnace (EAF) slag as an alternative construction materials to natural fine aggregates in concrete. By systematically evaluating the mechanical performance and observing general microstructural characteristics of concrete with different amount of slag replacement levels, this study provides some insights on the optimal amount of EAF slag should be use to maintain and improve material strength and quality. The findings from this study could provide some suggestions to mitigate the environmental concerns by encouraging the recycling of industrial by-products and this could further reduce the demand for natural resource extraction and minimizing landfill waste. This study also provides advantages from the prespective of economic by offering a cost-effective solution for the construction industry. This could have the potential to reduce the material costs while still improve the required qualities. This study also may contribute to the academic understanding of how different replacement ratios affect the overall concrete behavior. This in other way could contribute to the diverse of reference for future research and practical applications in developing greener and more sustainable construction materials.

1.7 Outline of the Report

This report comprises a total of five chapters regarding assessing the mechanical and microstructural properties of concrete with EAF slag replacement ratio of 60%, 75% and 90%.

The project's summary is provided in Chapter 1, which also includes information on the study's introduction, problems encountered, and byproducts produced in the existing steel manufacturing environment and other things. In

addition, the study's significance, problem description, goal, and target are covered. The study's scope and restrictions are then explicitly mentioned to state the limits and scope of the investigation. At the end of the chapter, the report's outline is also covered.

The study's literature review is illustrated in Chapter 2. This subject covers the overall concept of the mechanical properties and the one which focused in this study, types of slags available and replacement ratios used. Characteristics of steel slag is also being discussed here.

The approach and work plan to accomplish the goals are shown in Chapter 3. Material preparation, concrete casting and tests to carry out are being discussed in this chapter.

The test results and a discussion of the results are presented in Chapter 4. Based on SEM and EDX testing, the microstructure morphologies and elemental composition of the EAF slag are described. The stability and chemical composition of the concrete samples are also identified using the TGA and XRD tests respectively.

The experimental results are concluded in Chapter 5 which is also comes with suggestions for improving the accuracy of subsequent research.

CHAPTER 2

LITERATURE REVIEW

2.1 Introduction

CO_2 emissions had been an issue which is being highly aware by the peoples. One of the ways to reduce it is by utilizing the waste products from steel industries, which is the steel slag. Around the world, its utilization rate had reached near to 100% on certain developed countries such as USA, Japan, German and France (Yi *et al*., 2012). However, other countries had not reached this utilization rate but only achieved a lower rate. This maybe due to a lower awareness among the people of those countries about the benefits and usage of steel slag.

Steel slag can be used to reduce the amount of CO_2 by absorbing it into the slag and form carbonates. These carbonates are a stable form to be stored in it. Other than reduce the carbon dioxide emissions from the industry, steel slag is an environmental-friendly and sustainable material which is very useful to us. Produced as by-products during the steel manufacturing, it can be used as a replacement material in the concrete which also further strengthen its structural strength.

Types of slags will also be discussed since there are 3 types of slags, which are EAF slag, BOF slag, and LF slag. Concrete is one of the most widely used construction materials due to its versatility, strength and durability. In recent years, there has been increasing interest in incorporating industrial by-products such as Electric Arc Furnace (EAF) slag into concrete as a more sustainable alternative to natural aggregates. Previous studies have shown that the inclusion of EAF slag can influence both the mechanical and microstructural properties of concrete particularly its compressive strength which is a key indicator of performance. However, the effectiveness of slag incorporation largely depends on factors such as its chemical composition, particle size and the replacement ratio used. This study focuses on evaluating the compressive strength of concrete with partial replacement of fine aggregate using EAF slag at 60% 75%, and 90% replacement levels while also examining the underlying microstructural characteristics and factors that affect mechanical behavior.

2.2 Types of slags

Slag is a solid waste produced during the manufacturing of steel. Molten steel slags are subject to various methods of cooling; simple cooling, cooling with blasting water, cooling with water, cooling with air, and the shallow pool method. The most common method is that the slag is discharged in pools and cooled by blasting water. The slag is hardened when it encounters water and becomes a gray and low-porous material by crystallization. Approximately 400 kg of slag per ton is produced in iron and steel plants. It can further categorized into several types based on their steelmaking process respectively. It has a hard appearance and wear resistance due to its high Fe content. This make it difficult to experience losses on its material volume and has a long-lasting nature. It mainly consists of SiO_2, CaO, Fe_2O_3, FeO, Al_2O_3, MgO, MnO, and P_2O_5. These made up the chemical component of slags. However, chemical component of the slags varies with the furnace type, steel grades and pretreatment method. The main mineral phases contained in steel slag are dicalcium silicate (C_2S), tricalcium silicate (C_3S), RO phase (CaO-FeO-MnO-MgO solid solution), tetra-calcium aluminoferrite (C_4AF), olivine, merwinite and free-CaO (Yi *et al*., 2012).

2.2.1 BOF Slag

This type of slag is produced through the Basic Oxygen Furnace process which is being utilized in the steelmaking industry. It mainly uses iron ore as raw materials in the process. This process is usually incorporated with Basic Furnace (BF) process. During the BF process, molten metal would be the end product and would be fed into a BOF to lower down its carbon content. A high carbon content steel causes several defects such as inclusions and blowholes which form during solidification. Scrap metals are also added with the molten metal into the BOF, making up 20% to 30% of the entire charge. Oxygen is added into the charge to lead the formation of iron oxide and carbon monoxide which are exothermic reactions. The heat released by this oxidation process are favourable to the steelmaking process. Besides, lime and fluorspar are also added to form the slag. The slags produced here contains the impurities that are removed from the molten metal. This improves the purity of steel manufactured by BOF

(Naidu, Sheridan and van Dyk, 2020). The following Figure 2.1 further illustrates the concept of BOF in the form of schematic drawing.

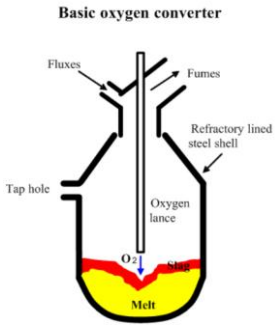

Figure 2.1: Schematic Drawing of Basic Oxygen Furnace (BOF) (Substech.com, 2012).

Chemical composition of BOF slags are varies based on different locations. This is due to the varying nature of the sources of ore and scrap used in the process. It has a high alkalinity due to the impurities which made up its contents. These impurities come from the ore and limestone which is added in during the process. CaO, MgO and slow dissolution of SiO_2 are these impurities. In these slags, the most abundant compound could be found are CaO and SiO_2. Magnesium oxide also have its presence in this type of slag. With the presence of the calcium and silicon compound such as previously mentioned, it gives this type of slag the ability of increasing the pH and alkalinity of solution. This is largely contributed by hydration of CaO by water molecules. Larnite, β-$Ca2SiO_4$ and different types of CaMg Oxides are also found in its chemical composition. For water which had been allowed to seep through this slag, it has the ability of leaching out certain elements. This is being defined as the mean toxicity characterization leaching potential (TCLP) of BOF-slags (Naidu, Sheridan and van Dyk, 2020). The amounts of chemical compounds of BOF slag from different countries can be refer on the following Table 2.1.

Table 2.1: Composition in % weight of BOF-S of varying particle sizes obtained from different sites (Naidu, Sheridan and van Dyk, 2020).

Country	Particle Size	Fe_2O_3	FeO	Fe met.	Al_2O_3	CaO	MgO	MnO	SiO_2	TiO_2	P_2O_5	Na_2O	K_2O	Cr_2O_3
Sweden (Tossavainen, Engstrom, Yang, & Menad, 2007)	30–40 mm	10.9	10.7	2.3	1.9	45	9.6	3.1	11.1	–	–	–	–	–
France (Windt, Chaurand, & Rose, 2011)	> 1 mm	29	–	–	2.5	40	5	6	13	–	1	–	–	–
France (Mahieux, Aubert, & Escadeillas, 2009)	0.04–1 mm	22.6	–	–	2	47.5	6.3	1.9	11.8	–	2.7	0.2	0.1	–
VOEST-VAI steel plant Austria (Chaurand, Rose, Olivi, Hazemann, & Proux, 2007)	> 2 mm	31.2	–	–	2.4	41.3	4.3	6.1	12.5	0.8	–	–	–	–
Kwangyang Iron & Steel Works plant in Korea (Sung Ahn, Chon, Moon, & Wong, 2003)	–	31.3	–	–	–	34.6	–	–	11	–	–	–	–	–
China (Yongjie Xue, Hou, & Zhu, 2009)	0.6 mm	17.8		–	6.8	45.4	7.3	–	13.7	–	–	–	–	–
India (Indian Bureau of Mines, 2016)	10 – 60 mm	16.50			1.07	50.70	10.31	1.05	17.69	–	–	–	–	–
India (Reddy, Pradhan, & Chandra, 2006)	–	16.2			1.3	52.3	1.1	0.39	15.3	–	3.1	–	–	0.2
South Africa (Doucet, 2010)	< 0.15 mm	16.5			3.4	41.2	8	4.3	18.8	–	1.3	–	–	–
South Africa (Doucet, 2010)	< 0.15 mm	17.3			2	49.9	7.7	1.2	16.9	–	0.3	–	–	–
South Africa (Doucet, 2010)	< 0.15 mm	26.9			7.5	38.1	9.4	3.2	13.9	–	1	–	–	–
Japan (Doucet, 2010)	< 0.15 mm	17.5			1.5	44.3	6.4	5.3	13.8	–	–	–	–	–
Finland (Doucet, 2010)	< 0.15 mm	24.1			1.8	43.6	1.4	2.4	13.9	–	–	–	–	–
USA (Brand & Roesler, 2015)	–	26.2			2.3	11	12.7	1.8	9.3	0.3	0.3	–	–	–

This type of slag can be exist in 3 structures, which are supercooled liquid, glassy or crystalline. Just as other substances, its physical properties are deeply affected by the chemical composition mentioned above and also the cooling method. The methods can be differentiated into water and atmospheric. Based on the speed of cooling under water, the lower speed yields a larger particle size of slag. Slag cooled under atmospheric has a harder and denser structure compared with the one cooled under water. Density of the particle of slag is in the range around 2.5 g/cm^3 and 3.6 g/ cm^3. High specific gravity and mechanical strength are also its characteristics. Just as the other type of slags, resistance on abrasion is applicable on BOF slags (Naidu, Sheridan and van Dyk, 2020). Further insights can also be refer to on the following Table 2.2.

Table 2.2: Physical Properties for BOF-S (Xue *et al.*, 2006).

Binder Adhesion (%)	Polishing stone value (%)	Crushing Value (%)	Pile Density (g/cm^3)	Bulk Density (g/cm^3)	Compressive Strength (N/mm^2)	Impact Value (%)	Water Absorption (%)	MOHS Hardness	Los Angeles Abrasion Loss (%)
> 95	57	12	1.92	3.29	200	17	1 – 1.18	7	13.1–17.6

2.2.2 EAF Slag

This type of slag has the similar process of production with BOF slag, but with the different way of heating the materials. At here, heat is added to the steel scrap and fluxes of limestone or dolomite by the electrodes which are extended into the furnace instead of supplying oxygen to yield an exothermic reaction in BOF. The electrodes carries electric current which turns into heat energy to melts the minerals. Fluxes used to remove silicates and phosphorus chemicals from the molten steel. Iron oxides react with the carbon present in the bath and

carbon monoxide gases are formed. Increase of CO gases causes the scrap melt starting to boil and the impurities being removed from the melt. The gaseous impurities escape and the liquid state remains as the slag. During stage of tapping, molten steel is drained from the furnace while slag is poured out from the slag door during superheating stage. Next, molten slag is solidified into a rock-like product via various cooling methods (Hosseini *et al.*, 2016). This process is further illustrated in the following Figure 2.2.

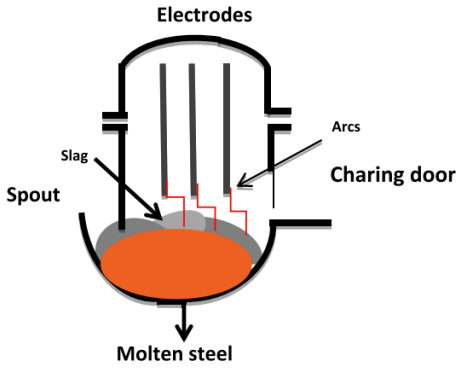

Figure 2.2: Electric Arc Furnace (Hosseini *et al.*, 2016).

EAF slag is produced in the value of 120–170 kg per ton of steel produced everytime. Similar with BOF slag, the chemical and physical properties of EAF slag varies based on the production plant. There are several factors which are affecting in these different plants, such as raw materials, different practices used in each of the factories, variations in the final products and differences in the slag treatments. Slags will still be produced as a waste products of steel making process but there will be variations presence. In this type of slag, the main components are iron oxides (FeO, Fe_2O_3), lime (CaO), silica (SiO_2), magnesia (MgO) and alumina (Al_2O_3). Other minor components are such as chromium, manganese, phosphorus oxides, and a little amounts of free lime is also found in it (Skaf *et al.*, 2017). This is being shown in the data of the following Table 2.3.

Table 2.3: Chemical composition of EAF slag (Skaf *et al.*, 2017).

	CaO	CaO_{free}	SiO_2	Al_2O_3	MgO	Fe_2O_3	FeO	MnO	P_2O_5	Cr_2O_3
(wt%)	25–35	0–4	10–20	3–10	2–9	10–30	7–25	<6	<6	<2

Similar as BOF slag, EAF slag have the appearance of rough, porous, rounded, blackish-gray aggregate and some small inclusions of metallic iron particles. It has a good shape with high angularity which can increase the ability of interlocking between particles. Density of this material is between the range of 3.2–3.8 g/cm^3. This material is very cohesive which makes it able to resist disintegration in a quite good way (Skaf *et al.*, 2017).

2.2.3 LF slag

This type of slag is the by-product of steel making industry which comes from further refining of molten steel after coming out of a basic oxygen furnace (BOF) or an electric arc furnace (EAF). It is being known as several names, such as basic slag, the reducing slag, the white slag, and also the secondary refining slag due to its applications in further refining (Rađenović, Malina and Sofilić, 2013). The process of further refining is also known as secondary metallurgy processes, which means that it is being reintroduced into the steel production process with varying amounts each time. It can be utilized in both BOF and EAF. The most important functions of the secondary refining processes are the final desulfurization, the degassing of oxygen, nitrogen, and hydrogen, the removal of impurities, and the final decarburization which is an important step for manufacturing the ultralow carbon steels. According to practices, the action of reintroducing can provides benefits on the characteristics of newly manufactured steels (Skaf *et al.*, 2016).

Since it is one of the 3 types of slags, its composition is almost similar with the 2 other slag but varies in the percentage available in it. For the chemical composition, the major compounds found are calcium, silicon, magnesium, and aluminium oxides, and calcium silicates under their various allotropic forms. The percentage of availability average of the chemical components are as following, where CaO is 35.54%; SiO_2 is 22.16%; Al_2O_3 is 11.65%; MgO is 13.83%; FeO is 2.53%; MnO is 0.48%; Cr_2O_3 is 0.15%; P_2O_5 is 2.35%; TiO_2 is 0.15%; K_2O is 0.57%; and Na_2O is 0.46%. All these values are determined by using the equipment which is the energy dispersive spectrometry (EDS) (Rađenović, Malina and Sofilić, 2013) and are shown in the following Table 2.4.

Table 2.4: Chemical composition of LF slag (Rađenović, Malina and Sofilić, 2013).

Slag Component	Wt%
CaO	48.37
SiO_2	15.00
FeO	1.54
Al_2O_3	14.30
MgO	15.25
Na_2O	0.43
K_2O	0.36
TiO_2	0.20
P_2O_5	2.73
Cr_2O_3	0.92

2.3 Overview of Concrete with EAF Slag

Electric Arc Furnace (EAF) slag is a by-product being produced during the production of steel in the Electric Arc Furnaces. This industrial waste material contains large quantity of Calcium Oxide (CaO), Silicon Dioxide (SiO_2), Iron Oxides (Fe_2O_3) and other minerals. These compounds makes the EAF slag become a potential alternative to natural aggregates in concrete casting. The physical characteristics of EAF slag such as high density, angular shape and rough texture could provide the benefits in mechanical interlocking within the cement matrix. These surface characteristics could further improve the bonding between the aggregate and cement paste which important in improving compressive and flexural strength in concrete (Pellegrino and Gaddo, 2009).

Some research from previous have studied on the mechanical performance of concrete with EAF slag as replacement for fine aggregates. Research which had done by Manso *et al.* (2006) found that replacement levels around 50% to 75% could get a higher compressive strength than control mixes. This improvement was achieved by better aggregate-cement paste adhesion. However, when the replacement level exceeds a certain limit such as 90% issues such as the poor workability and volume instability have the probability to happen. Maslehuddin *et al.* (2003) showed that EAF slag content in excess

amount may causing expansion and cracking due to the free lime (CaO) and Magnesium Oxide (MgO) which hydrate and expand over time.

From the perspective of microstructural properties, EAF slag which contained in the concrete tends to show a denser internal matrix with reduced porosity. This can be found out in the microscopic images of the sample through SEM. This denser structure can lead to improved durability, reduced permeability and improve the long-term performance. Tsakiridis *et al.* (2008) had observed that utilizing of slag in concrete could promote the formation of secondary Calcium Silicate Hydrate (C-S-H) phases. This is a favourable condition when slag is used in optimal proportions. Energy-Dispersive X-Ray (EDX) analysis detects increased amount of calcium and silicon which are crucial elements in hydration reactions. In the study which had been carried out by (Qasrawi *et al.*, 2009), they had further concluded that the presence of these elements are the activities of active hydration and contributes to strength development.

Other than the mechanical and microstructural advantages, the use of EAF slag in concrete also aligns with sustainable construction goals. This method of replacing natural aggregates with industrial by-products which is the slags could reduce the demand for quarrying, conserves natural resources and minimize the issue of handing the steel manufacturing waste.

In a nutshell, concrete with incorporating of EAF slag had showed beneficial properties in mechanical, microstructural and environmental. This could be optimised if the replacement ratios is being set at moderate replacement levels. However, further detail controlling of replacement ratios and proper processing of the slag are still required and important to avoid durability issues and ensure quality assurance in concrete uses.

2.4 Mechanical Properties of Concrete

Concrete had been commonly used in construction due to favourable mechanical properties such as high compressive strength and moderate tensile strength. Conventional concrete achieves the mechanical strength mainly by forming the Calcium Silicate Hydrate (C-S-H) gel during the hydration of cement. This component is the primary binding compound in the concrete. Compressive strength of normal concrete usually has the range of 20 MPa to 50

MPa for the general applications. However, the compressive strength yielded also still based on the mix design, curing conditions and the water-cement ratio (Neville, 2011).

For concrete with the incorporation of Electric Arc Furnace (EAF) slag, several research had reported similar or improved mechanical properties especially at moderate replacement levels. Most of the research stated that this is due to the rough texture and angular shape of EAF slag particles, this could further strengthen the bonding between aggregates with cement paste. This results in better load transfer within the concrete matrix. According to (Pellegrino and Gaddo, 2009), concrete with EAF slag as the replacement for fine aggregate at the ratio of 50% to 75% could achieved higher compressive strength than control mixes due to improved interfacial transition zones and denser packing between the particles.

Study from (Manso *et al.,* 2004) had found that EAF slag could improve the compressive and tensile strength of concrete. This is due to the high density and potential pozzolanic contribution from compounds such as CaO and SiO_2. The pozzolanic reaction helps to produce additional C-S-H gel which could strengthen the concrete microstructure as this is the main binding component in concrete. After 28 days, EAF slag concrete with the 65 to 75% replacement ratio of EAF slags as fine aggregate had showed improvements in compressive strength for 15% higher than conventional concrete.

However, at higher replacement levels such as 90% and above the mechanical properties may decrease. This is due to the increment of water demand and potential volume instability from free lime which did not hydrate and MgO. In the study conducted by (Maslehuddin *et al.*, 2003) they had observed that excessive amount EAF slag content could reduce workability which could cause segregation and further reduce the compressive strength. They reported that after the replacement ratio of 75%, the mechanical performance will decrease unless there are some adjustments in the mix proportions such as adding superplasticizers or supplementary cementitious materials.

For the context of flexural strength, EAF slag concrete has shown improved performance compared to conventional concrete. The rough and angular texture of slag particles had provide beneficial characteristics which is

help to anchor the cement paste and distribute the stress applied more efficiently across the concrete matrix. Research which had done by Qasrawi *et al.* (2009) had reported that the flexural strength of EAF slag concrete had increases for approximately 10% at the 50% slag replacement concrete compared to control mixes.

For splitting tensile strength, EAF slag concrete had similar and improved results compare to conventional mixes. This is obviously observed when replacement ratios used are being optimized. The improved microstructure and reduced porosity had helped in contributing to better crack resistance and tensile stress distribution (Qasrawi *et al.*, 2009).

As summary, concrete incorporating with EAF slag shows mechanical properties that are equal to or exceeds the conventional concrete. The studies recommended that for replacement ratios which is controlled within the range of 50% to 75% could be the optimise choice to achieve improved mechanical strength. Both types of concrete also depends on C-S-H formation as the primary source of strength and both can achieve comparable performance if these concretes are mixed with appropriate mix proportions and curing practices. However, optimizing the further mix ratio is still needed at higher slag replacement levels to avoid compromising in mechanical properties.

2.5 Factors affecting Mechanical Properties

After having some introduction to the concept of mechanical properties of concrete, factors which could affect the mechanical properties are vital to ensure the results of concrete yield could be optimised. Based on the studies, the mechanical properties of concrete incorporating with specific replacement ratio of Electric Arc Furnace (EAF) slag are influenced by several factors which also affecting each other at the same time such as replacement level, particle size and shape, chemical composition, water demand, workability and curing conditions. These factors determine the overall strength, durability, and structural integrity of the concrete matrix.

One of the most critical factors is the replacement ratio of natural EAF slag as the fine aggregate. At moderate replacement ratio which is at the range between 50% and 75%, this ratio of EAF slag replacement has been reported to have the effect of improving the compressive and tensile strength. This

improvement is due to the increased particle interlock and strengthen bonding formation at the Interfacial Transition Zone (ITZ) which also contributed by the rough and angular texture of slag particles at the same time. However, when the replacement level exceeds a certain level which is usually around the ratio of 75%, the workability and compaction of the mix had been observed to decrease which causes poor cohesion and increasing of voids in the matrix which could further reduce the mechanical strength (Pellegrino & Gaddo, 2009).

Another significant factor which is the chemical composition of EAF slag used in the replacement. Large amount of free Lime (CaO) and Magnesium Oxide (MgO) which exist in the slag can causes delayed expansion and cracking which could produce negative effect in concrete's long-term strength and durability. However, if the slag added into the mix is properly processed by stabilizing the free Lime (CaO) and Magnesium Oxide (MgO), these components can act as pozzolanic or hydraulic materials in the cement matrix. Silicon Dioxide (SiO_2) which is left in the slag and stabilized Calcium Oxide (CaO) can react with water and existing Calcium Hydroxide ($Ca(OH)_2$) which can contribute to secondary hydration by forming additional Calcium Silicate Hydrate (C-S-H) gel (Manso *et al.*, 2006). This could further enhance the strength of the concrete (Manso *et al.*, 2006).

Water-cement ratio is another important factor which affects the mechanical strength. Due to the high porosity and absorption characteristics of EAF slag which can be usually found in unprocessed or coarsely crushed form, concrete with this type of EAF slags tend to require more water which can in turn increases the effective water-cement ratio if not properly adjusted. This effect of dilution could reduce the density of the hardened paste and adversely affect the compressive strength (Qasrawi *et al.*, 2009).

Particle grading and fineness also affect the packing density of concrete. Slag aggregates with good grade could fill the voids efficiently, improve the compressive strength and reduce permeability. Poor grading or oversized particles may affect the interfacial bond and create weak zones which reduce the overall mechanical strength.

Curing conditions also play a vital role in strength development of mechanical properties. Since incorporation of EAF slag may cause variations to the hydration process, curing process with the suitable moisture content could

ensure the reaction being carried out continuously and prevents shrinkage happens due to early dry which is more concerning for using EAF slag at high replacement levels. Extension of curing time may significantly improve early strength development in EAF slag concrete due to prolonged pozzolanic and filler effects (Aldea *et al.*, 2000).

2.6 Microstructural Properties of Concrete with EAF Slag

The microstructural properties of concrete plays a vital role on influencing its mechanical performance especially the compressive strength. In the context of concrete incorporating Electric Arc Furnace (EAF) slag as a partial replacement for fine aggregate, understanding the elemental and compound composition could provides valuable insight into how is strength-related behavior. Key elements such as Calcium (Ca) and Silica (Si) influences in modifying the microstructure of concrete at both early and later stages of curing especially when slag is introduced into the mix.

Calcium which is commonly present in both cement and EAF slag is essential for the development of a dense and cohesive binder phase. High calcium content enhances early-age reactivity which promotes the rapid formation of binding phases that fill the internal pore network. This contributes to early densification of the microstructure which is crucial for initial strength gain. Calcium's presence could reduce capillary porosity by promoting reaction with water and other reactive oxides. Well compacted internal structure with fewer voids causes better load-bearing capacity and compressive strength. Studies by (Pellegrino and Gaddo, 2009) and (Manso *et al.*, 2004) observed that slag mixes with higher Ca concentrations show more compact microstructures and stronger performance under compression.

Silica contributes to the improving of pore structure and long-term microstructural stability. Sufficient silicon amount encourage the formation of dense gel-like phases that fill voids and microcracks in the matrix. This action improves the homogeneity of the paste and strengthens the internal skeleton of the hardened concrete. Silicon also enhances the microstructural continuity between aggregate and paste which can improve the stress distribution under load. The presence of Si in elemental analysis has positively impact with

compressive strength outcomes in slag-modified concrete as shown by study of (Tsakiridis *et al.*, 2008).

Formation of Calcium Carbonate ($CaCO_3$) through carbonation reactions can also influence microstructural characteristics. When Carbon Dioxide from air reacts with available Calcium Hydroxide in the matrix, $CaCO_3$ is formed and it can fill pores and cracks within the paste. This effect contributes to increased surface hardness and local densification which may enhance compressive strength under specific curing and exposure conditions. While excessive carbonation may reduce pH and durability, controlled $CaCO_3$ formation especially in calcium-rich mixes can be beneficial in strengthening the near-surface region. Studies by (Ngala and Page, 1997) confirmed that partial carbonation could reduce porosity and improve the compactness of the cement matrix.

In short, Calcium, Silica and Calcium Carbonate formed which contain in the microstructure of concrete with EAF slag help reduce porosity, improve bonding and strengthen the internal structure of the concrete which could lead to better compressive strength.

2.7 Focusing on Compressive Strength for Mechanical Properties

Compressive strength is commonly recognized as the most fundamental and important mechanical properties in concrete research and structural design. It directly shows the load-bearing capacity of concrete and is commonly used to classify and specify concrete grades such as C25, C30 and C40 in construction standards. This parameter serves as the basis for evaluating the suitability of concrete in structural applications such as columns, slabs, beams and foundations. The main function of the concrete is to withstand the compression load applied and this is also the main advantageous of concrete materials. Compressive strength testing is standardized and provides reproducible results which makes it a practical and effective measure for comparing different concrete mixes (Neville, 2011).

Fine aggregates which usually is the natural sand serve an essential function in concrete by filling voids between coarse aggregates, enhancing particle packing and contributing to the density and homogeneity of the mix. They influence the strength and durability of the hardened product of concrete.

The texture, grading, shape and surface area of fine aggregates play a significant role in the development of the interfacial transition zone (ITZ) between aggregate particles and the cement paste. A denser and more cohesive ITZ results in better load transfer and higher compressive strength. When conventional fine aggregates are replaced with EAF slag which generally shows the characteristics of rough, angular texture and higher specific gravity, the packing density and mechanical interlock can be enhanced. This could produce a denser microstructure and improved stress distribution which can positively affects compressive strength (Pellegrino & Gaddo, 2009) and (Manso *et al.*, 2004).

In addition to physical characteristics, the chemical composition of the cementitious matrix also impacts compressive strength. One important compound is Calcium Carbonate ($CaCO_3$) which is commonly formed through the carbonation of Calcium Hydroxide ($Ca(OH)_2$) which is a by-product of cement hydration. This reaction occurs when atmospheric Carbon Dioxide (CO_2) penetrates the concrete and reacts with $Ca(OH)_2$. Formation of $CaCO_3$ can have both beneficial and reduction effects on compressive strength depending on the duration and location of carbonation. On one hand, $CaCO_3$ can fill pores and microcracks which could increase the density and surface hardness of the concrete. This could contributing modestly to strength development. On the other hand, excessive carbonation may reduce the alkalinity of the concrete matrix which potentially weakening the long-term stability of hydration products such as Calcium Silicate Hydrate (C-S-H) and compromising the protection of steel reinforcement (Ngala & Page, 1997).

Focusing studies on compressive strength in this study could be supported with the microstructural analysis component of the study. The use of characterization techniques such as Energy Dispersive X-ray Spectroscopy (EDX) and X-Ray Diffraction (XRD) enables evaluation of elemental composition and hydration products such as Calcium (Ca), Silica (Si), and Aluminum (Al) compounds. These elements play a critical role in the formation of Calcium Silicate Hydrate (C-S-H) which is the main strength-contributing compound in concrete. Since C-S-H affects the compressive strength, analyzing the relationship between composition chemistry and strength performance could provide insights for this study. This integrated approach allows the study to

focus on informative and mechanical property that reflects the influence of both physical and chemical characteristics of EAF slag.

2.8 Replacement Ratio of EAF Slag utilized in this study

In recent years, there has been a growing interest in utilizing Electric Arc Furnace (EAF) slag as a partial replacement for fine aggregate in concrete. Several studies have been conducted to assess its mechanical performance especially the compressive strength across varying replacement ratio. However, the findings remain mixed and depend on specific replacement ratio, material properties and experimental conditions used. Studies such as (Qasrawi *et al.,* 2009) and (Chadee *et al.,* 2025) reported modest or inconsistent improvements in compressive strength at low replacement levels (<50%) indicating that lower substitution may not be sufficient to fully exploit the beneficial characteristics of EAF slag. On the other hand, research by (Manso *et al.,* 2004), (Pellegrino and Gaddo, 2009) and (Mekonen *et al.,* 2024) demonstrated peak performance in compressive strength at moderate replacement levels (50 to 75%) due to improved particle packing, enhanced interfacial bonding and better hydration reactions. Studies that examined high replacement ratios (>75%) such as (Behforouz *et al.,* 2025) and (Maslehuddin *et al.,* 2003) often highlighted either a decline in strength or lack of sufficient data and showing challenges such as increased water demand, workability loss and potential microstructural weaknesses.

As studied by (Manso *et al.,* 2004) and (Pellegrino and Gaddo, 2009), these studies identify this moderate range (50 to 75%) as optimal for strength development due to the slag's rough texture and favorable physical properties. The inclusion of a 60% replacement level in the current study could provides insights on whether the findings from previous studies still suitable as this current studies utilizes EAF slags with different particle size. This variable may affect the result obtained from current study but could provide more information to future reference.

The 75% replacement level serves as a critical threshold for assessing whether performance benefits continue or begin to diminish. Recent studies such as (Manso *et al.,* 2004) noted that strength increases may plateau or begin to reverse beyond moderate levels. Including 75% in this study allows for the

investigation of performance near this upper moderate limit which contributing valuable data on mechanical and microstructural properties.

The 90% replacement level is selected to explore the high substitution part as (Maslehuddin *et al.*, 2003) highlighted that high slag content (>75%) may lead to reduced compressive strength and increased workability or durability challenges due to high water demand and potential volume instability. However, evaluating the 90% replacement ratio can provides critical insights into the material limits of EAF slag usage and feasibility for using more sustainable concrete. This aligns with calls in research for more data on high-substitution mixtures which are important for maximizing industrial waste utilization in green construction.

It is crucial to note that variations in testing conditions including mix design, curing regime, slag processing method and fineness limit the direct comparability of findings across studies. These inconsistencies may contribute to the scattered and sometimes conflicting conclusions observed in the literature. Therefore, to contribute to a more continuous understanding of how EAF slag replacement affects compressive strength, current study focuses on 3 strategically chosen replacement levels which are 60%, 75% and 90%. These values represent the moderate-to-high range where previous studies have either reported peak strength, noted performance thresholds or lacked conclusive data. By evaluating compressive strength and microstructural characteristics using consistent testing methods, this study could clarify trends and offer new insights into the practical application of high-volume EAF slag in concrete.

2.9 Particle Size Range of EAF Slag utilized in this study

The particle size of Electric Arc Furnace (EAF) slag significantly influences the mechanical and microstructural properties of concrete. Finer particles such as those in the range of 0.8–2.36 mm offer a larger surface area, improving the hydration process and leading to a denser microstructure which can improve compressive strength. However, coarser particles in the range of 4.75–6.30 mm may result in weaker interfacial bonding and increased porosity if not properly graded. Medium-sized particles in the range of 2.36–4.75 mm usually provide a balance between workability and strength.

According to ASTM C33, the 4.75 mm sieve which also known as sieve No. 4 serves as the standard threshold differenciating fine and coarse aggregates. Materials passing through this sieve are classified as fine aggregates while those didn't are considered as coarse. This classification is crucial for concrete mix design as the proportion of fine and coarse aggregates affects the workability, strength and durability of the concrete.

Study done by (Li *et al.*, 2023) shows that finer steel slag particles improe the compactness of concrete by filling pores more effectively which leading to improved mechanical properties. The study found that the smaller the particle size of steel slag, the better the gelling activity and the denser the structure which causes superior mechanical performance.

By selecting particle size ranges that containing both sides of the 4.75 mm standard which are 0.8–2.36 mm, 2.36–4.75 mm, and 4.75–6.30 mm, this study could comprehensively observe the influence of EAF slag particle size on concrete properties. This approach aligns with standard classifications and could provide insights of how different particle sizes impact the performance of slag-modified concrete.

2.10 Analytical Method

2.10.1 Thermogravimetric Analysis (TGA)

This analysis is use in thermal field where the change in weight of the substance is recorded as a function of temperature or time. Some parameters such as purity, composition and absorbed moisture contents etc. can be measured by excuting this analysis. It has 3 types of TGA, which are Static, Quasistatic and Dynamic. Each of them are chosen based on the temperature setting required (Bimal Raut, 2022).

This analysis kick started with heating the sample substance. The initial weight of this sample substance is being recorded prior heating. During the heating process, heating temperature is being increased at various time intervals, such as 5 minutes, 10 minutes and 15 minutes. During each different temperature level, the changes of weight for sample substance is being recorded. Results of TGA can be presented as a thermogravimetric curve (TG curve). This curve presents the results by recording the weight changes as a function of temperature or time. In the curve, horizontal portions represents regions where

there is no weight loss while the curved region in the vertical portion indicates weight loss. Weight changes is being priorotized as the parameters to present as results is due to physical changes and the building and breaking of chemical bonds at high temperatures. Each subsances has its unique TG curve due to different molecular structures. For the temperature ranges, 0-1200°C is the common range for this analysis (Bimal Raut, 2022). This is being further illustrated in the following Figure 2.3.

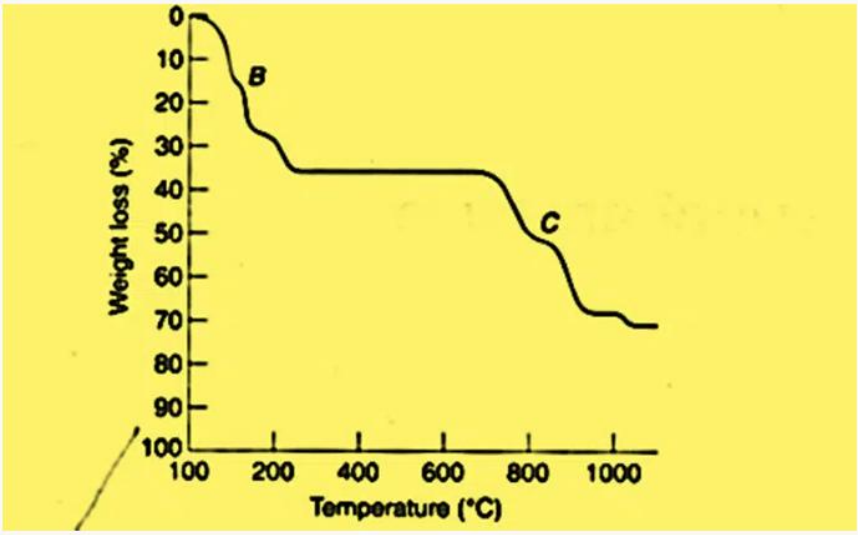

Figure 2.3: Typical TG curve for $CuSO_4.5H_2O$ (Bimal Raut, 2022).

Major components required for TGA are as following such as balance, furnace assembly (which containing sample container, temperature sensor, furnace liner, thermocouple), recorder and display, purge gas system which is use to provide an inert atmosphere and etc. The key components are balance and the furnace assembly to run this analysis (Bimal Raut, 2022). The concept is being further illustrated in the following Figure 2.4.

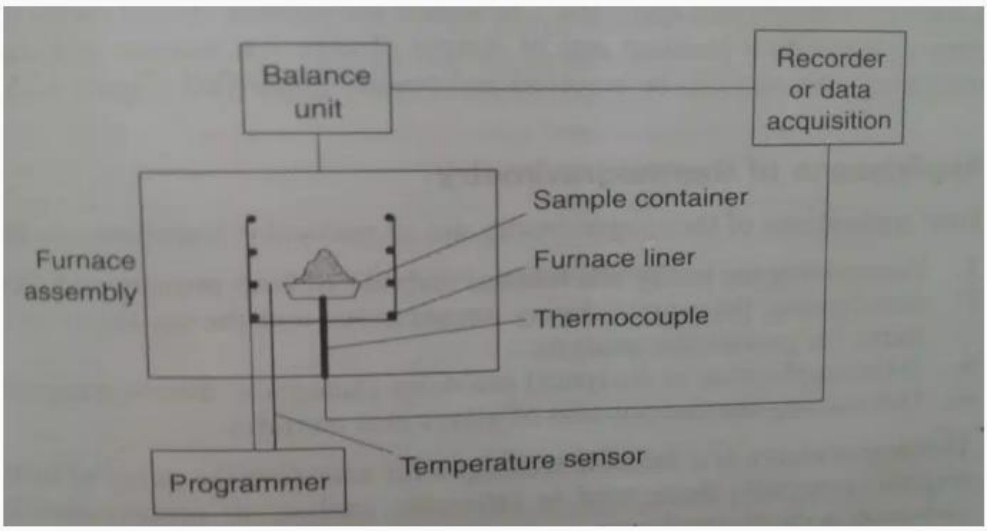

Figure 2.4: Diagram of TGA Instrumentation (Bimal Raut, 2022).

TGA is matched to the title of this study, which is the carbonation of steel slags. As CO_2 is being sequestered into the slags, this analysis can provide a medium to determine the composition of substance since this is one of its applications. This analysis could also let the researchers to study on the ideal drying temperatures and the appropriateness of different weighing methods for TGA. This analysis is known for its rapid processing, short cooling time and a high accuracy of balance which is available inside its apparatus (Bimal Raut, 2022).

2.10.2 Scanning Electron Microscopy (SEM) Analysis

This analysis is actually using a large microscope which comes with electronic devices and electrons support. It is a type of electron microscope that scans surfaces of sample substances by using a beam of electrons which are moving at low energy. This can let the electrons to focus and scan the specimens detailly and clearly. It is more different from the conventional type of microscopes, which usually utilizing light. Images of microstructure of the sample substance which are taken from the conventional light microscope are not clear and sharp due to it has an inefficiency and longer wavelengths. Electron microscopes which using electron beams with shorter wavelengths eneables a more precise and better resolution power (Mokobi, 2020).

This analysis works on the principle of application of kinetic energy. These energies are being utilized to produce signals on the interaction of the

electrons. There are several electrons involved, such as secondary electrons, backscattered electrons, and diffracted backscattered electrons. These electrons are functioning to provide view of crystallized elements and photons. Among the three electrons mentioned earlier, both secondary and backscattered electrons are used to produce image for the user. The secondary electrons which are being emitted from the specimen play the primary role of detecting the morphology and topography of the specimen while the backscattered electrons produce the contrast in the composition of the elements of the sample substance which are being put in earlier (Mokobi, 2020). All these functions happens under vacuum conditions. This condition could prevents molecules or atoms which are already exist in the microscope column from interacting with the electron beam. This interaction may reduce the high resolution of image that are being expected to form initially (SciMed, 2023).

SEM analysis could be utilized in many fields. This is due to its user-friendly interfaces and easily operatable. Even new user could use it easily. Effieicncy could also be increased drastically as it only requires around 5 minutes to obtain data from the analysis. These fields includes industrial uses, nanoscience studies, biomedical studies, microbiology and etc. The images which are provided from SEM analysis usually covers these three pillars, which are topography, composition and morphology. Distribution of features or parts on a surface of a sample is being included in the topography of the sample while composition shows what a sample is made of. For morphology, it is the form and shape or structure of the provided sample. The main types of analysis are Backscattered Electron Detection (BSE), Cathodoluminescence (CL) and Electron Backscatter Diffraction (EBSD). For BSE, it produces the images that carries the information on the composition of the sample. It lets the user to know how is it like in the internal part of sample and what forms the sample. CL is very useful in researching of luminescent materials as it could produces high-resolution digital images of the materials which comes with this properties. While for EBSD, direct information about crystalline structure, orientation of materials and polycrystalline aggregates are provided by SEM (SciMed, 2023).

2.10.3 X-Ray Diffraction (XRD) Analysis

This analysis utilize the technique which is common to most people in the analysis which is the X-Ray. X-Ray is common due to its existence in the hospitals which is being use to generate the internal images of the patient's body. It helps the doctors to have a view on the place where the human eyes can't reach. In the situation here, this techniques is being used on the materials. It is use to determine the crystallographic structure of a material and orientation of powder, solid and liquid samples by irradiating a material with X-rays and measures the intensities and scattering angles of the X-rays that leaving the material to go to the machine that emits it. It is quite similar to the SEM Analysis which is being mentioned earlier. By using this technique, the sample does not need to be changed or damaged in order to be analyzed (drawellanalytical, 2023).

This analysis operates based on the constructive interference of monochromatic X-rays and a crystalline sample which is expected to be studied. X-rays are an radiation wave which is electromagnetic properties. It comes with a wavelength that is similar to the spacing between atoms in crystals of the sample. When the beam of the X-rays is being focused at a crystal from the apparatus, the X-rays get contact with the electrons in the atoms. As these electrons are scattered everywhere in the atoms, the X-Rays are being diffracted in different directions. Since every materials have its unique arrangement of atoms, the diffraction pattern could be utilized in the determination of the crystal structure (drawellanalytical, 2023).

This analysis could be used at many fields due to one of its properties which is non-destructive. It does not destroy or causes damages to the sample when it is being analyzed. Therefore, any valuable or fragile samples which are expected to study its internal structures can be done by utilizing this analysis mechanism. With regards to the same properties of non-destructive, this analysis perform versatility and universality. Same as the X-Rays machine which is common in the hospitals, this analysis could be found easily at any laboratories and research institutions around the world (drawellanalytical, 2023).

2.10.4 Energy Dispersive X-Ray Spectroscopy (EDX) Analysis

This analysis has a few names which are EDXS and EDAX. Each of them also refer to the same thing, which is EDX analysis. It is use to identify and quantify

the elements present in a sample substance. This analysis is being used together with the SEM analysis. It can identify the elements available in the sample after the sample being scanned through the SEM apparatus. This analysis expose the sample with a focused electron beam. This causes the the atoms from the sample to emit characteristic X-rays. Since every element in the sample has different atoms, these X-rays are being emitted at an unique energy levels which are unique to that element. Therefore, by analyzing these emitted X-rays, this analysis can determine the existence and abundance of elements which are within the sample and present it in different colours (Thermofisher, 2024).

The concept of elemental mapping is being utilized in this analysis. It is a technique which is used to generate the image of how is the distribution of elements inside a sample. These images provides a detailed view of how different elements are distributed. This provide a medium for the users to have more understanding on the sample's internal structure. Elemental mapping are generated by combining the information collected during the analysis of either SEM EDS. The details such as point-to-point info are being utilized here. Every elements have its respective colours which are being pre-determined. In the image of elemental map, there is colour difference could be observed obviously. These colour scale represents the concentration of certain element at the respective points. The brighter the colours, the higher the concentrations of the element at that point or vice versa (Bruker, 2024).

Similar with SEM and XRD analysis, EDX analysis is also known for its universality and non-destructive properties. This makes it applicable to almost all the susbtance that are expected to be determined for its internal components and structures. The sample can be reused and it increase the effectiveness since it does not require a new one for every analysis. During the analysis, EDX provides both qualitative and quantitative information about the elemental composition of a sample substances. This includes the major and minor elements, trace elements and impurities which exist in the sample. The time required for obtaining the results from the analysis is short and could provide real-time info which is vital for experiments (Thermofisher, 2024).

2.11 Summary

This literature review part had highlighted the growing environmental concern regarding CO_2 emissions and the potential of steel slags especially the Electric Arc Furnace (EAF) slag as sustainable construction materials. While being utilized commonly in developed countries, the steel slags offer some core benefits such as environmental management through carbon sequestration and enhanced concrete performance when used as aggregate substitutes.

Three primary types of steel slag which are Basic Oxygen Furnace (BOF), Electric Arc Furnace (EAF) and Ladle Furnace (LF) slag are introduced with detailed explanations of their production processes, chemical compositions and physical characteristics. Slags are emphasized due to its high content of calcium, silica and iron oxides. This makes them suitable for partial replacement of fine aggregates in concrete.

Several studies show that EAF slag improves concrete's mechanical and microstructural properties such as compressive strength when replacement ratios range between 50% and 75%. At optimal levels, benefits are such as improved particle interlock, enhanced hydration and denser microstructures. However, high replacement levels such as 90% can reduce workability and cusing durability challenges due to the presence of unhydrated free lime and Magnesium Oxide.

Microstructural advantages of EAF slag concrete are linked to high calcium and silica content which promote the formation of strength provider which is the Calcium Silicate Hydrate (C-S-H) gel. Controlled carbonation also contributes positively by densifying the matrix through Calcium Carbonate formation. Compressive strength is identified as the primary performance parameter due to its relevance in structural applications and standardization in concrete classification.

The review also identifies key factors which influencing the mechanical performance such as replacement ratio, particle size, chemical composition, water-cement ratio and curing conditions. Particle size is investigated in this study with ranges from 0.8–6.30 mm to evaluate both fine and coarse effects based on ASTM C33 standards.

Finally, four analytical methods which are Thermogravimetric Analysis (TGA), Scanning Electron Microscopy (SEM), X-Ray Diffraction

(XRD) and Energy Dispersive X-Ray Spectroscopy (EDX) are discussed as critical tools for characterizing the thermal, elemental and structural properties of EAF slag concrete. These methods support the investigation of strength development and microstructural behavior under various slag replacement ratios and particle sizes.

CHAPTER 3

METHODOLOGY AND WORK PLAN

3.1 Introduction

Figure 3.1 in this chapter provides an overview of the process which had been used in this study. The creation of the sample which was using EAF steel slag, cement, water and sand were the first stage of the investigation. Prior the sieving, oven dry for EAF slags had being carried out. The EAF slag particles are sieved by using 7 sieving pan with specific sizes of openings and 1 final pan to further categorize it into the 3 particles size ranges. Sand and cement were also being sieved. After finish preparing the raw materials required, concrete mixing and casting works were carried out with the partial replacement of EAF slags. The concrete samples which were cast in the plastic mould were left for air curing for 24 hours and water curing for at least 28 days. After this, the concrete samples were placed into the Compressive Strength Machine to determine the compressive strength of the sample. Samples are being further crushed into powder form to carry out the test of SEM, EDX, XRD and TGA to further study the mechanical and microstructural properties of concrete samples with EAF slag replacement ratios of 60%, 75% and 90%.

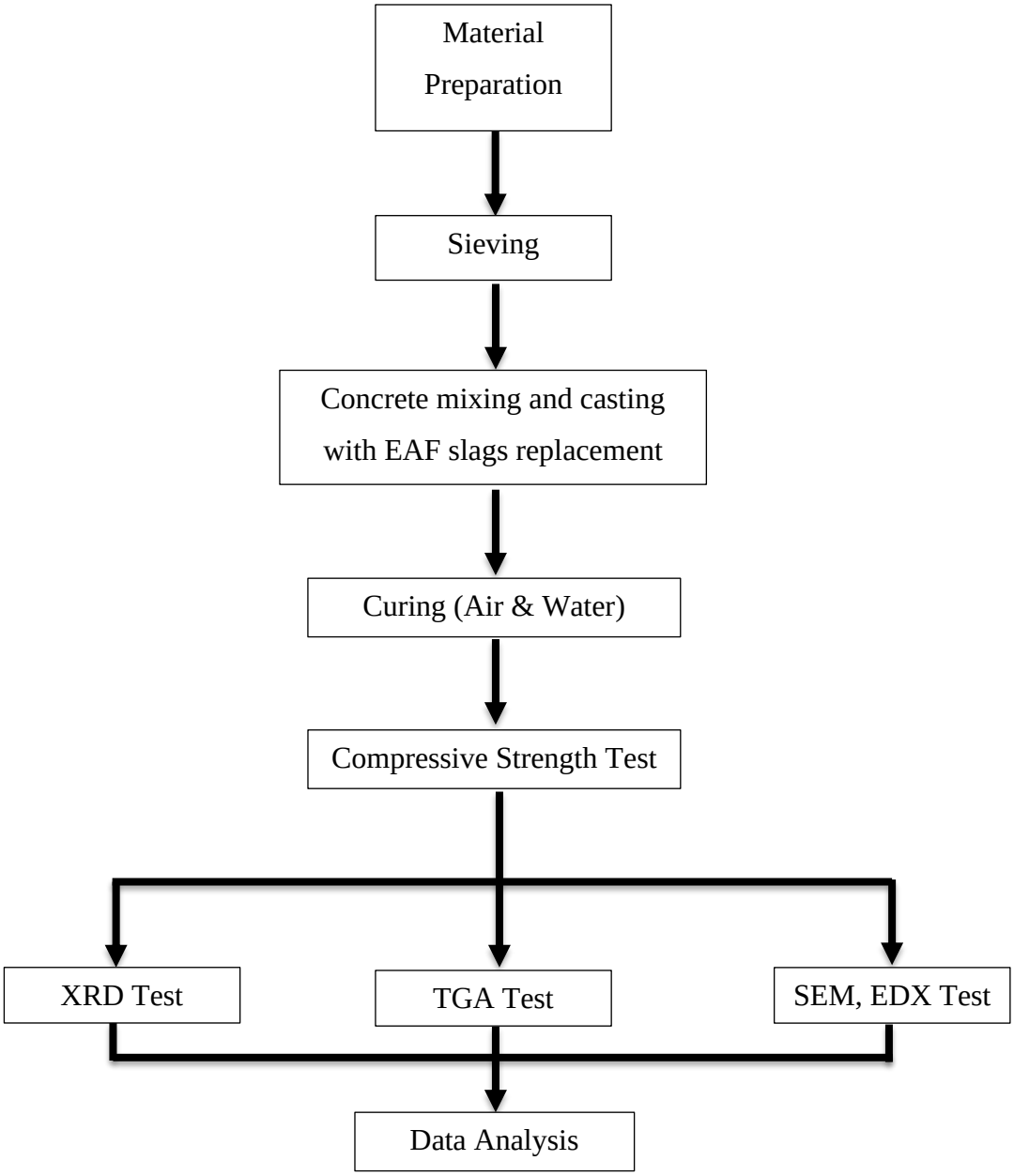

Figure 3.1: Process of Methodology.

3.2 Materials Preparation

Penang-based Electric Arc Furnace (EAF) slag was required before the concrete casting process can be kick started. Steel slag is a powder that is obtained from the steel industry as a by-product and is as shown in Figure 3.2. The Penang-based Electric Arc Furnace (EAF) slag used in this study is the steel slag as mentioned earlier. In order to make sure the EAF slag is dry and free of excess water, it was dried in an oven for at least a day at a temperature between 100-110°C before being sieved and used for replacement in concrete mixing and casting. This preparation aligns with recommendations for sample conditioning prior to aggregate testing in ASTM C136/C136M Standard Test Method for Sieve Analysis of Fine and Coarse Aggregates. The oven dry of the EAF slag is as shown in the following Figure 3.3. The EAF slag which had been chosen for this study are being categorized into 3 particle size range.

Figure 3.2: Sample of EAF Slag.

Figure 3.3: Oven dry of EAF Slags.

Other than the preparation of EAF slags, the other raw materials which also required in this study were such as Ordinary Portland Cement (OPC), water and sand which act as the fine aggregate. The Ordinary Portland Cement (OPC) which being used in this study was the “Cap Buaya Cement” manufactured by Tasek Cement which is as shown in Figure 3.4. Each of the package was came with 25 kg per bag. Fine aggregate which is the sand was also prepared in this stage which is as shown in Figure 3.5. Water was an essential component in the mixing process . To ensure the quality is preserved, the municipal tap water was utilized for all mixing procedures in this research. The water used was as shown in the following Figure 3.6.

Figure 3.4: Ordinary Portland Cement (OPC) used for concrete casting.

Figure 3.5: Sand used for concrete casting.

Figure 3.6: Water used for concrete casting.

3.3 Sieving

EAF slag was used for the sieving process through the sieves as shown in the following Figure 3.7. The weighted EAF sample was placed on the top sieve with 6.3 mm, 5 mm, 4.75 mm, 3.35 mm, 2.36 mm, 2 mm and 0.8 mm sieve sizes arranged in top to bottom order. The sequence used was in line with ASTM C136/C136M or BS EN 933-1 Tests for geometrical properties of aggregates Part 1: Determination of particle size distribution – Sieving method. These sieves were being categorized into 3 particle size ranges which were 0.8-2.36mm, 2.36-4.75mm and 4.75-6.3mm. Next, the cover plates were tightened and the entire sieve was set up on the sieve shaking machine. The sieve shaking machine was being operated for 10 minutes. The EAF slag sieve arranngement was as shown in Figure 3.7. The slags particles which left on the sieves and the final pan were being placed into different containers respectively based on the particles sizes ranges. These containers were being labelled properly to prevent misleading information happens.

Figure 3.7: EAF Slag Sieve Arranngements.

3.4 Concrete Mixing and Casting

In these concrete casting works, a total of 36 samples were being cast. As mentioned earlier, there are 3 particle size ranges which were 0.8-2.36mm, 2.36-4.75mm and 4.75-6.3mm being set in this study. Each of the particle size range had 3 different particle size ranges and each of these ranges had 3 samples. These 3 samples were intended to provide a more reliable and accurate results as this made average results exist. Among these 30 samples, 1 set with total 3 samples act as the control while the other 9 sets with total 27 samples were based on different particle size ranges and replacement ratios of EAF slags. To further illustrate the samples, the following Table 3.1 and Table 3.2 can be referred.

Table 3.1: Quantities of Concrete Samples in this study.

Replacement Ratios of EAF Slags	**Particle Size Ranges**		
	0.8mm to 2.36mm (R1)	**2.36mm to 4.75mm (R2)**	**4.75mm to 6.3mm (R3)**
60%	3	3	3
75%	3	3	3
90%	3	3	3

Table 3.2: Naming of Concrete Samples.

Replacement Ratios of EAF Slags	**Particle Size Ranges**	**Naming**
0%	-	Control/Normal Concrete
60%	0.8mm – 2.36mm	R1_EAF_60%
75%	0.8mm – 2.36mm	R1_EAF_75%
90%	0.8mm – 2.36mm	R1_EAF_90%
60%	2.36mm – 4.75mm	R2_EAF_60%
75%	2.36mm – 4.75mm	R2_EAF_75%
90%	2.36mm – 4.75mm	R2_EAF_90%
60%	4.75mm – 6.3mm	R3_EAF_60%
75%	4.75mm – 6.3mm	R3_EAF_75%
90%	4.75mm – 6.3mm	R3_EAF_90%

Mixing proportion of each raw materials were vital during this stage. This proportion also plays an important role for the strength developed after the concrete being cast later. A markup of 20% was included for each raw materials proportions to provide a buffer for wastage. In calculation of the mixing proportion, the absolute volume method had been utilized here. In the proportions, a water-cement ratio of 0.55 had been used for both water and cement materials. Mixing and casting procedures were conducted in accordance with ASTM C192/C192M Standard Practice for Making and Curing Concrete Test Specimens in the Laboratory. In the following Table 3.3 and Table 3.4, the mixing proportions for both normal concrete which was the control and concrete sample with 60% EAF slag replacement under R1 particle size range were being shown out.

Table 3.3: Mix Proportion of Normal Concrete (Control).

Raw Materials	**Proportions (%)**	**Mass (kg)**
Sand	39.28	11.012
Water	21.61	6.058
Ordinary Portland Cement	39.30	11.015
Total	≈ 100	≈ 28.039

Table 3.4: Mix Proportion of Concrete Sample R1_EAF_60%.

Raw Materials	**Proportions (%)**	**Mass (kg)**
Sand	14.08	3.951
Water	19.36	5.433
Ordinary Portland Cement	35.22	9.878
EAF Slag	31.34	8.792
Total	≈ 100	≈ 28.054

After calculated the mixing proportions of each raw materials required for the concrete sample casting, all raw materials as mentioned above were measured and weighed before the mixing process start. Before starting the mixing, OPC, EAF slag and Sand were poured into the mixer except water. Figure 3.8 illustrated the pouring of OPC while Figure 3.9 showed the pouring

of EAF slag into the mixer. Pouring of water was as shown in the following Figure 3.10. These 3 materials were dry-mixed prior adding in water. After that, water was added slowly while the mixing still carry on. Measurement for the density of fresh concrete was carried out to ensure complying on the required standard. This procedure was repeated for mixes which are using different EAF slag replacement ratios of 60%, 75% and 90%. For the control, the procedures were also similar but only excluding the steps of adding in EAF slags.

Figure 3.8: Pouring OPC into the mixer.

Figure 3.9: Pouring EAF slag into the mixer.

Figure 3.10: Pouring water into the mixer.

After the mixing works completed, these mixed raw ingredients which had turned into the concrete were used for casting the concrete samples. The mixed materials were being poured into the plastic moulds. These plastic moulds were in the cube shape with the dimensions of 150 mm × 150 mm × 150 mm. This was following the standard mould size specification in BS EN 12390-1 Testing hardened concrete - Part 1: Shape, dimensions and other requirements for specimens and moulds. Before the casting, oil was being applied inside the moulds with a thin layer by using a brush. This was to let the concrete sample more easier to be removed on the next day. A small paper label was placed at the bottom of each mould to help identify the samples. The pouring were carried out in 3 levels of volume. When the concrete poured reached certain levels, the pouring was stopped and a tamping rod was used. This is to remove the trapped air bubbles and prevent segregation which have the potential to cause impact on the mechanical strength. Figure 3.11 illustrated the pouring of concrete into the moulds. Filled moulds were then left to set and harden at the laboratory for 24 hours which was the air curing. This was as shown in the following Figure 3.12. After 24 hours, the concrete sample in the mould was removed by using the compressed air. The removed samples were then labelled prior placing them in the curing tank for at least 28 days. The curing in the water tank is to provide a platform to promote good cure. Figure 3.13 illustrated this step. These were in line with BS EN 12390-2 Making and curing specimens for strength tests. After at least 28 days, the samples were removed form the curing tank for further analysis by carried out the tests as mentioned earlier. The removed samples were being air dried for 24 hours before carry out the compression strength test.

Figure 3.11: Pouring concrete into plastic moulds.

Figure 3.12: Concrete in moulds left to set and hardened (air curing).

Figure 3.13: Placing concrete samples in curing tank.

3.5 Compressive Strength Test

The next step involved was to determine the compressive strength of the concrete sample. This test was carried out by using a compression testing machine. Before the testing started, the concrete sample had to be inspected for ensuring the sample was remain in an undamaged condition. The cross-sectional area of the sample was then measured. To perform the test, the cube was placed at the center-below of the machine's hydraulic press to ensure compression pressure from the machine was effectively transmitted to the sample. The platen where the sample was located inside the machine was cleaned before inserting the sample. The machine then applied pressure to the cube until the sample cracked as shown in the following Figure 3.14. The highest load that the sample could withstand was recorded as the compressive strength of the sample. All these were in accordance with BS EN 12390-3 Testing hardened concrete - Part 3: Compressive strength of test specimens. Cross-sectional area measurement and platen alignment were ensured before loading. After that, the sample was taken out and crushed into smaller particle sizes using a hammer. All these smaller particles were collected in a small ziplock plastic bags and labelled properly based on the sample names respectively as showed in Figure 3.15. This action was to prepare these slags to do SEM, EDX, XRD and TGA tests accordingly.

Figure 3.14: Sample in Compresison Strength Machine.

Figure 3.15: Samples collected in small ziplock plastic bag.

3.6 SEM and EDX Test

To produce a high resolution image, the surface morphology and microstructure of materials can be examined by using Scanning Electron Microscopy (SEM) which was a good imaging tool. Through the application of a concentrated electron beam, SEM generates high-resolution and detailed pictures that enable

the observation of features at nanoscale level. To further improve its capabilities, SEM could be combined with Energy-Dispersive X-Ray Spectroscopy (EDX) to generate the elemental analysis of the material.

In order to assure equipment compatibility and prevent interference with the SEM examination, EAF slag is crushed into smaller particles and placed on the pin stubs. The pin stubs was as shown in the following Figure 3.16. The specimens were kept within a 15mm height and size range. The samples were then put into the Hitachi S-3400N SEM machine as shown in Figure 3.17. With the incorporating of computer software, a range of 1500× to 3000× image magnification was utilized in order to investigate the microstructure of carbonated EAF slags. The surface topography, shape, size and distribution of particles can all be characterized with the use of SEM.

The elemental composition of the samples was determined by using the Energy Dispersive X-Ray (EDX) Test as an tracing method after the SEM examination was finished. The tracing focuses on elements such as Magnesium (Mg), Calcium (Ca), Aluminum (Al) and others. In order to analyze the samples, contact between X-ray and a sample was required. These released X-rays indicated whether or not the sample contained the elements that are being focused. The device for EDX Test is incorporated together with the SEM machine and could be found in the following Figure 3.17.

Figure 3.16: Pin Stubs to contain samples for SEM and EDX Test.

Figure 3.17: Machine for SEM Test and EDX Test.

3.7 XRD Test

X-ray diffraction (XRD) was a non-destructive technique used to examine a material's crystalline structure with the objective of identifying the metal compounds, crystalline structure and minerals present in a solid substance. The powdered EAF slag sample was produced and placed on the sample holder prior to being placed inside the XRD apparatus for analysis. This was being illustrated in the following Figure 3.18. The machine used to carry out this test was as shown in the Figure 3.19. Regarding the scanning procedure, the scattering angle (2Θ) varies between 5° and 85°, required a 40-minute waiting period and a scanning rate of 2° per minute. This was consistent with ASTM D7348 or ASTM E1126 Standard Guide for Evaluating Non-metallic Crystalline Materials by X-ray Diffraction. After that, the reflections of the scanning zones produced the spectrum which includes particular mineral components contained in the carbonated slags. The "Search Match" button was used in order to determine which mineral compound matched the peak shown in the spectrum. To find the best match, the input spectrum was being compared to the software's library of mineral components.

Figure 3.18: Crushed samples on the holder prior insertion.

Figure 3.19: Machine for XRD Test.

3.8 TGA Test

Thermogravimetric analysis which was also being known as the TGA test was a technique that includes tracking a sample's mass as it was exposed to different temperatures. TGA analysis measured changes in mass under regulated heating or cooling settings to provide important insights into the composition, thermal stability and decomposition kinetics of materials. The EAF slag sample in this study was heated under controlled conditions which was ranging from 25°C to 900°C by using a constant weight monitoring system. This system operates at a rate of 10°C per minute. Nitrogen gas (N_2) was used as a carrier gas with a constant flow rate of 50 ml/min and a purge gas flow rate of 20 ml/min to prevent the oxidation of the EAF slag sample during heating. This setup referred to ASTM E1131 Standard Test Method for Compositional Analysis by Thermogravimetry. Mass changes over time or a function of temperature were recorded to create the Thermogravimetric Curves (TG Curve). The apparatus used for this test was shown in the following Figure 3.20.

Figure 3.20: Apparatus for TGA Test.

3.9 Summary of Chapter

In a nutshell, the goal of this study is to investigate the mechanical and microstructural properties of concrete with EAF slag replacement. EAF slags partially replace the fine aggregate in concrete. These slags were sieved by using 6.3 mm, 5 mm, 4.75 mm, 3.35 mm, 2.36 mm, 2 mm and 0.8 mm sieve. A total

of 36 slag samples were cast. After that, SEM and EDX analysis were carried out to find out the sample's microstructure by SEM machine and the element composition of the slag sample by using EDX analysis. To identify the crystalline structure which were contained in the sample, XRD test was also carried out. Finally, to find out the stability of the sample at various temperatures, TGA test was also being carried out.

CHAPTER 4

RESULTS AND DISCUSSION

4.1 Introduction

This chapter shows the results of tests which had been done under this study and discuss the explanations on the results obtained. These tests are such as Compression Strength test, SEM test, EDX test, XRD test and TGA test. All these tests aims to provide valuable observations and results for the applications of EAF slag and to achieve the aim and objectives of this study.

For the Scanning Electron Microscopy (SEM) test, this test uses electron beams which had been focused to generate high-resolution image to identify the surface topography, shape, size and distribution of particles on the sample surface. These generated images could provide a valuable insight to study on these structures formed on the surfaces.

For Energy-Dispersive X-ray Spectroscopy (EDX) test, this test is usually being utilized together with SEM test. By using the focused electron beams from SEM on the sample's surface, the elemental composition of the samples could be obtained by the EDX machine. These elemental compositions are being measured in the terms of weight percentage.

While for X-ray Diffraction (XRD) test, this test analyse the sample's crystalline structure with the objective of identifying the chemical compounds present in the sample. This analysis uses X-rays to get contact with the sample. The results obtained can help to provide the information on the arrangement of both atoms and molecules in the sample.

For Thermogravimetric Analysis (TGA) test, this test is for the determination of weight for the samples which varies under a period of time. This test is being carry out under different temperatures in a controlled time period. This analysis provide valuable results into the composition, thermal stability and decomposition of the samples.

For Compression Strength test, this test aims to analyse the compression strength of concrete which mixed with EAF slag. This could help to study on the effect of slags which had been mixed into the concrete on the mechanical strength which is being focused on compression strength.

4.2 Concrete being Cast Under Various Material Conditions

In this study, a total of 30 samples had been casted under different conditions. These conditions are the varies particle size and replacement ratio of EAF slag being used when casting the concrete. These samples are being used to determine the optimal replacement ratio of EAF slag. Table 4.1 below shows a total of 30 samples which being used.

Table 4.1: Various Material Conditions for Concrete Casting.

Particle Size Range (mm)	Name of Range	Replacement Ratio (%)	No. of Concrete Cast (cubes)
0.80-2.36	R1	60	3
		75	3
		90	3
2.36-4.75	R2	60	3
		75	3
		90	3
4.75-6.3	R3	60	3
		75	3
		90	3
-	-	0	3

Particle size range of EAF slag which being used are increasing from R1 to R3 which have the range from 0.8mm to 6.3mm. Replacement ratio of slags in concrete is increased with 15% from 60% to 90%. The No. of concrete casted for each category is being set as 3 cubes per category as this is to get an average value on the test which being carry out. Average value could let the results obtained to be more accurate and reliable.

4.3 Energy-Dispersive X-ray Spectroscopy (EDX) Test

In this section, the analysis of Energy Dispersive X-ray Spectroscopy (EDX) Test is being used and under general conditions this test is being carried out with Scanning Electron Microscopy (SEM) Test to determine and investigate the information of sample's elemental composition which is crucial when studying and analyzing the microstructural properties of the samples. Calcium (Ca) and Silicon (Si) are the 2 vital elements in contributing to the strength development of concrete especially the formation of C-S-H gel during hydration process. As EDX test could provide information on elemental composition, the amount of Calcium and Silicon which available could be obtained and further utilized to study how these amounts affect the strength development which is compressive strength in this study. This could link the findings which obtained in this part to achieve one of the objective which is to study the elemental and chemical compound composition which affect the compressive strength of concrete with EAF slag replacing fine aggregate at ratio of 60%, 75% and 90%. High and sufficient amount of Calcium and Silicon could ensure and improve the effectiveness of C-S-H gel formation. EDX analysis could generates the result based on the X-rays that reflected from a sample after it is subjected to electrons emission. In this study, samples of different particle size range of EAF slags which are R1 (0.8 mm - 2.36 mm), R2 (2.36 mm - 4.75 mm) and R3 (4.75 mm - 7 mm) with different replacement ratio of 60%, 75% and 90% respectively were prepared and being analyzed under this EDX test.

Table 4.2: Elemental Composition of Elements Available in Concrete with EAF Slags Replacement Ratios of 60%, 75% and 90%.

Particle Size	Replacement Ratios (%)	Elemental Composition in At%					
		Carbon (C)	Oxygen (O)	Magnesium (Mg)	Aluminum (Al)	Silicon (Si)	Calcium (Ca)
R1	60	27.96	45.37	1.04	1.75	6.66	21.98
	75	7.98	57.79	1.76	2.24	8.26	29.10
	90	4.27	53.96	1.74	2.78	8.14	36.36
R2	60	7.35	60.98	1.74	1.43	6.81	30.83
	75	18.58	49.35	1.68	4.78	7.44	20.47
	90	37.92	39.25	1.78	2.04	4.66	17.23
R3	60	6.56	53.38	1.62	1.38	6.24	21.70
	75	8.66	57.94	1.52	2.76	8.65	18.17
	90	4.70	48.10	2.32	1.77	6.74	14.35
Control		1.39	15.82	1.25	3.86	13.83	49.85

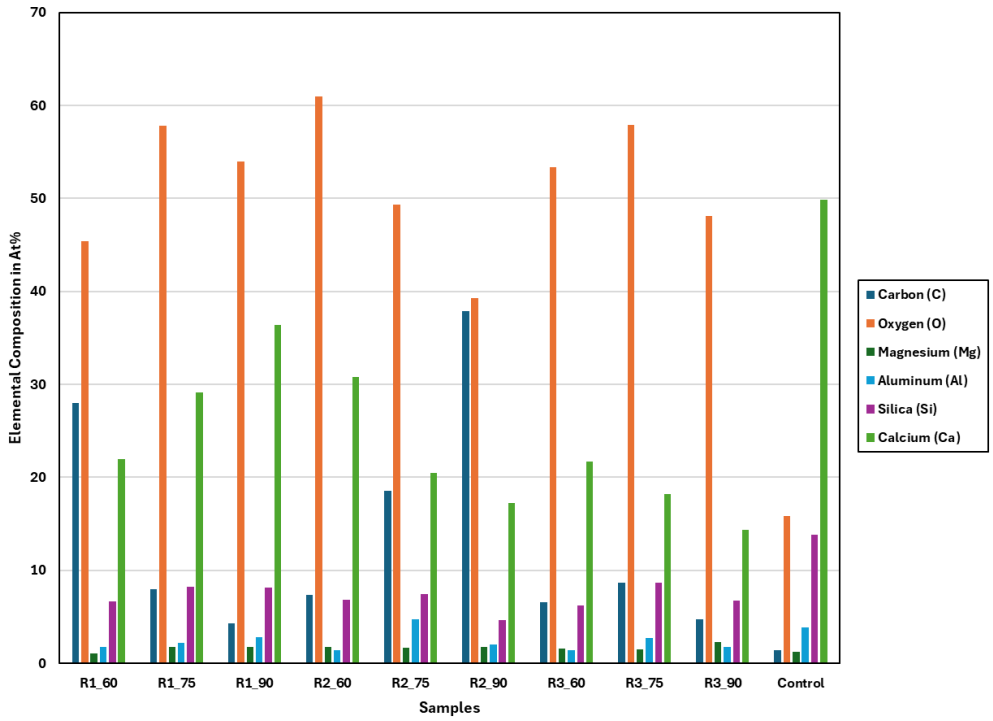

Figure 4.1: Elemental Composition of Concrete Samples under Different Particle Size and Replacement Ratio.

Based on the data shown in the above Table 4.2 and Figure 4.1, these informations of Elemental Composition in the unit of Atomic Percentage (At%) are being studied to investigate the microstructural properties which could affect the compressive strength. Data from Table 4.2 are being presented again in Figure 4.1 to have a better visual on the changes of quantity in each elemental composition. In the EDX Test, there are several elements being determined which are Carbon (C), Oxygen (O), Magnesium (Mg), Aluminum (Al), Silicon (Si) and Calcium (Ca). Each of these elements have their roles respectively on contributing to the mechanical properties of the samples which focus on compressive strength especially for Silicon (Si) and Calcium (Ca) but for the elements such as Carbon (C), Oxygen (O), Magnesium (Mg) and Aluminum (Al) their contribution may not significant. These elements are being studied as they are often to be observed for their presence in slag concrete samples.

By referring to the data in Figure 4.1, there are some observations can be made by analyzing the elemental composition of EAF slag concrete data and its effect on compressive strength which is one of the important components of mechanical strength for concrete samples. Aluminum element is found to have highest level at concrete sample of R2 75% and control while the lowest level at concrete sample of R2 60% and R3 60%. As Aluminum element contributes in the early strength of concrete via Ettringite structure, this result shows the impact of different structural properties and potential performance under different EAF slag replacement ratio and particle size. The following element is Magnesium. Based on the results, the concrete sample of R3 90% have the highest amount of Mg while concrete sample of R1 60% have the lowest amount of Mg recorded. Although both samples had been incorporated with specific replacement ratio of EAF slags at different particle sizes, this shows the potential impact of Magnesium element on structural integrity and durability as concrete sample of R1 60% have higher compressive strength than concrete sample of R3 90%. In terms of Oxygen, concrete sample of R2 60% have the highest level recorded while concrete sample of R2 90% have the lowest level recorded. This observation shows that although under the similar particle size but deviation of element content may still exist. For Carbon element, the concrete sample of R2 90% have recorded the largest level while the concrete sample of R1 90% have recorded the lowest level of Carbon. This difference

brings out the potential impact on the carbon sequestration capacity which could have the chance to affect the environmental sustainability.

Calcium plays a critical role in strength development as it is necessary for hydration reactions and the formation of binding compounds. The analysis showed that R1 samples has a steady increase in calcium content with higher replacement levels which is 21.98% at 60%, 29.10% at 75% and 36.36% at 90%. This observation shows that finer EAF slag particles at higher replacement contribute more calcium, enhancing cementitious bonding and compressive strength. In contrast, R2 samples had the highest Ca content at 60% which is 30.83% but experienced a significant drop at 75% which is 20.47% and further at 90% which is 17.23%. This indicates that while moderate amounts of medium-sized slag can improve strength, excessive replacement may reduce the availability of calcium and weaken the structure. R3 samples displayed generally low and decreasing calcium levels which is 21.70% at 60%, 18.17% at 75%, and 14.35% at 90%. This shows that coarser particles release less calcium and are less effective in supporting hydration which could reduce the compressive strength.

Silicon also plays an important role in the development of microstructure by contributing to matrix densification. It reduces porosity and enhances particle packing especially when supported by sufficient calcium. In the R1 samples, silicon content increased with higher slag replacement by small reduction which are 6.66% at 60%, 8.26% at 75% and 8.14% at 90%. These combined with the high calcium levels shows the strong potential for compressive strength due to improved matrix compaction. R2 maintained moderate silicon content across all replacement levels which are 6.81% at 60%, 7.44% at 75% and 6.06% at 90%. However, the declining silicon and calcium at higher replacement levels may cause looser internal structure and reduced strength. Interestingly, R3 samples showed the highest silicon content at 75% which is 8.65% but this was accompanied by low calcium which is 18.17%. The lack of sufficient calcium may have limited the strength development and at 90% both Silicon (6.74%) and Calcium (14.35%) were relatively low which could causes weaker structural performance.

In short, the results from EDX analysis demonstrate that calcium and silicon content affects compressive strength in concrete with EAF slag. Higher calcium supports better hydration and early bonding while sufficient silicon enhances the density and continuity of the matrix.

4.4 X-ray Diffraction (XRD) Test

In this test, XRD analysis is radiating the material with X-ray emitted by the machine. The intensities and scattering angles of X-ray being diffracted by the crystalline structure existed in samples are being presented in the graphs which could be analyzed by X'Pert HighScore Plus Software. In the analysing of the software, the results shows that the samples matches with some of the chemical compounds from the Crystallography Open Database. The main compounds which can be found in the concrete samples are such as Magnesium Oxide (MgO), Calcium Carbonate ($CaCO_3$), Calcium Hydroxide ($Ca(OH)_2$), Silicon Dioxide (SiO_2), Calcium Sulfate Hydrate ($CaSO_4.2H_2O$) and Calcium Oxide(CaO). The composition of chemical compound for the concrete sample could be determined under this test. These data could be further study and analyze for the microstructural properties of the samples. Calcium Hydroxide ($Ca(OH)_2$) and Calcium Carbonate ($CaCO_3$) are the by-products and products of hydration and carbonation process respectively. Although Calcium Carbonate is produced through carbonation process but within the controlled amount it still have the functions of filling the pores and matrix densification which is crucial for strength development. Excessive amount is unfavourable. For Calcium Hydroxide although it plays the role as by-product which is formed when Tricalcium Silicate (C_3S) and Dicalcium Silicate (C_2S) of cement reacts with water, it still crucial as it maintain a high pH or alkalinity environment which is important to maintain the chemically stability of main strength contributing component such as C-S-H gel and also crucial compound to produce additional C-S-H if supplementary cementitious materials like fly ash or silica fume is added as they need $Ca(OH)_2$ to react with it for further development. The amount of these 2 compounds which is part of the compositions obtained could be further study on how it affects the compressive strength of concrete with EAF slag replacement. Excessive amount of Calcium Carbonate could reduce the efficiency of hydration by consuming $Ca(OH)_2$

before it can form C-S-H while for Calcium Hydroxide is due to remained unreacted due to the lack of available silicon. However, low amount of Calcium Hydroxide could causes low alkalinity environment and destabilize the C-S-H gel which is crucial for strength development while for low amount of Calcium Carbonate it would be lesser matrix densification which is unfavourable for strength development. Throughout the study in this test, this could link the findings which obtained in this part to achieve one of the objective which is to study the elemental and chemical compound composition which affect the compressive strength of concrete with EAF slag replacing fine aggregate at ratio of 60%, 75% and 90%. By using this software, this further simplifies the determination process of the existed chemical compounds and provides important information on their existing percentages. The information of each available chemical compounds can be found in the following Figure 4.2 and Figure 4.3.

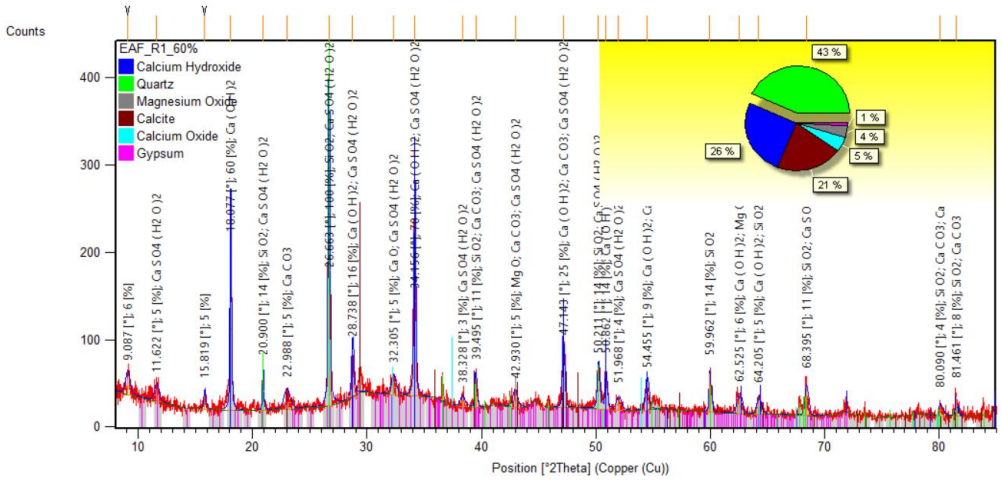

Figure 4.2: XRD analysis for R1_EAF_60% concrete sample.

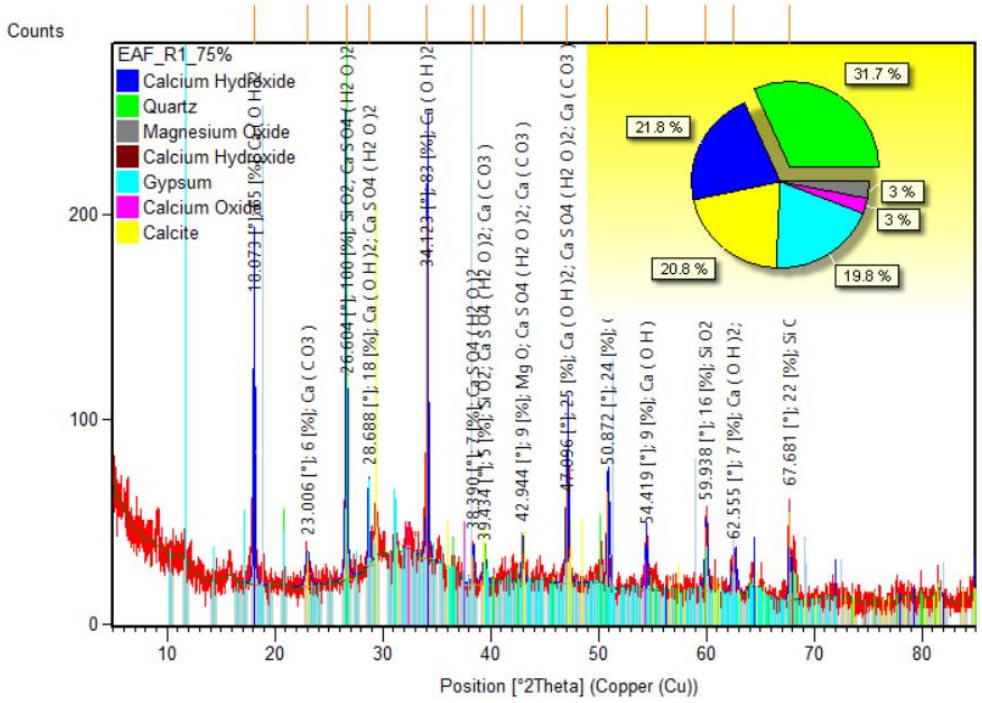

Figure 4.3: XRD analysis for R1_EAF_75% concrete sample.

Based on the informations shown in the above Figure 4.2 and 4.3, the chemical composition for each of the identified 6 chemical compounds in terms of Wt% can be obtained. All of these informations are being summarized and included in the following Table 4.3.

Table 4.3: Summarized Information of Each Identified Chemical Compounds from Concrete Samples.

Concrete Sample	Compound	Quantitative Percentage (Wt%)
EAF_R1_60%	MgO	4.0
	$CaCO_3$	21.0
	$Ca(OH)_2$	26.0
	SiO_2	43.0
	$CaSO_4 \cdot 2H_2O$	1.0
	CaO	5.0
EAF_R1_75%	MgO	3.0
	$CaCO_3$	20.8
	$Ca(OH)_2$	21.8

	SiO_2	31.7
	$CaSO_4 \cdot 2H_2O$	19.8
	CaO	3.0
EAF_R1_90%	MgO	7.5
	$CaCO_3$	0
	$Ca(OH)_2$	29.1
	SiO_2	60.5
	$CaSO_4 \cdot 2H_2O$	1.74
	CaO	1.16
EAF_R2_60%	MgO	0.0
	$CaCO_3$	2.0
	$Ca(OH)_2$	5.1
	SiO_2	90.9
	$CaSO_4 \cdot 2H_2O$	0.0
	CaO	2.0
EAF_R2_75%	MgO	4.0
	$CaCO_3$	2.0
	$Ca(OH)_2$	24.8
	SiO_2	55.4
	$CaSO_4 \cdot 2H_2O$	10.9
	CaO	3.0
EAF_R2_90%	MgO	7.0
	$CaCO_3$	5.0
	$Ca(OH)_2$	72.0
	SiO_2	10.0
	$CaSO_4 \cdot 2H_2O$	1.0
	CaO	5.0
EAF_R3_60%	MgO	0.0
	$CaCO_3$	6.0
	$Ca(OH)_2$	20.0
	SiO_2	42.0
	$CaSO_4 \cdot 2H_2O$	27.0

	CaO	5.0
EAF_R3_75%	MgO	0.0
	$CaCO_3$	0.0
	$Ca(OH)_2$	1.0
	SiO_2	99.0
	$CaSO_4 \cdot 2H_2O$	0.0
	CaO	0.0
EAF_R3_90%	MgO	6.0
	$CaCO_3$	50.0
	$Ca(OH)_2$	32.0
	SiO_2	12.0
	$CaSO_4 \cdot 2H_2O$	0.0
	CaO	0.0
Control	MgO	10.0
	$CaCO_3$	26.0
	$Ca(OH)_2$	13.0
	SiO_2	30.0
	$CaSO_4 \cdot 2H_2O$	21.0
	CaO	26.0

This test is being conducted on 30 concrete samples which including 27 samples with Electric Arc Furnace (EAF) slag replacements at different ratios of 60%, 75% and 90% while another 3 control samples without any slag replacement. This test highlighted differences in the presence and proportions of specific crystalline compounds. Among these compounds, Calcium Carbonate ($CaCO_3$) and Calcium Hydroxide ($Ca(OH)_2$) are being focused as they play vital roles in contributing to the development of mechanical properties for concrete with EAF slag replacement which is compressive strength. Although Calcium Hydroxide ($Ca(OH)_2$) did not contribute directly but it is plays a supporting roles in the hydration process which is crucial for strength development. Therefore, highlighting this compound is important as it affects stability of the hydration process.

Silicon Dioxide (SiO_2) had been frequently found in the samples with high composition such as 91% in EAF_R2_60% and nearly pure which is 99.0% in EAF_R3_75%. In concrete, SiO_2 generally acts as a filler with the function to fill up the spaces within the concrete to improve strength and durability by reducing voids and porosity. For most of the conditions, SiO_2 is inert which means that it doesn't react actively and chemically. However, if SiO_2 is existing in a very fine size, this compound becomes reactive which also known as Fine Reactive Form. SiO_2 can then take part in chemical reactions with Calcium Hydroxide to produce additional binding materials which could enhance the concrete strength and durability (Siddique & Bennacer, 2012).

Next, Calcium Sulfate Hydrate which also known as Gypsum ($CaSO_4 \cdot 2H_2O$) had also varied significantly by reaching as high as 27.0% in sample of EAF_R3_60% but is completely absent in samples such as EAF_R2_60%, EAF_R3_75% and EAF_R3_90%. In general, Gypsum helps to control the setting time of cement by avoiding the concrete from hardening too quickly. However, excessive amounts of gypsum could cause sulfate attack which leads to unfavourable expansions and cracking. This also causes the weakening of concrete (Skalny *et al.*, 2002).

Magnesium Oxide (MgO) had been observed to only having difference in small amounts in the samples but it reached as high as 10% in the control sample. MgO in limited quantities can improve the stability of concrete by helping it overcome the changes in volume over time. However, excessive amounts of MgO can cause delayed expansions which may leading to cracks and compromised structural integrity (Mo *et al.*, 2014). Similarly, Calcium Oxide (CaO) which also known as Lime remained at a low quantity of 0 to 5% throughout the samples. This shows the little risk of expansion or instability may caused by the lime. However, the effects of this compound should not be ignored for quality assurance and optimal purpose.

Compressive strength of concrete is related to its chemical composition and the hydration products that form. Among the compounds identified through XRD analysis, Calcium Hydroxide ($Ca(OH)_2$) and Calcium Carbonate ($CaCO_3$) are important due to their direct links to hydration efficiency and microstructural development. When interpreted the composition from EDX especially Calcium

and Silicon content together with this analysis the behavior and strength outcomes of each mix can be better understood.

Calcium Hydroxide forms as a result of the reaction between cement and water and its presence reflects the progress of hydration. Moderate or Moderate-to-high levels of $Ca(OH)_2$ typically indicate that hydration is active and that strength development is ongoing especially when there are sufficient silicon to react with the $Ca(OH)_2$ and form Calcium Silicate Hydrate (C-S-H). However, if $Ca(OH)_2$ accumulates in large amounts without being consumed, it may indicate an imbalance in the mix that limits further hydration and potentially weakens the concrete matrix.

In the R1 series, EAF_R1_60% and EAF_R1_75% shows $Ca(OH)_2$ contents of 26.0% and 21.8% respectively. Both mixes also showed reasonably high Si contents which are 6.66% and 8.26% and also the notable calcium levels from EDX analysis which are 21.98% and 29.10% respectively. These values shows that hydration was proceeding actively with a balanced chemical environment that encouraging the conversion of $Ca(OH)_2$ into strength-giving products. EAF_R1_90% showed a moderate to high $Ca(OH)_2$ content which is 29.10% and high Calcium and Silicon from EDX which are 36.36% Ca and 8.140% Si. This showing the strong hydration potential and minimal carbonation as the data shown is 0% $CaCO_3$. This combination may could supported a denser microstructure and higher compressive strength.

In contrast, EAF_R2_90% recorded an excessively high $Ca(OH)_2$ content of 72.0%. The EDX results showed a relatively low silicon content (4.66%) showing that much of the $Ca(OH)_2$ in this sample may have remained unreacted due to the lack of available silicon. This imbalance could reduced formation of C-S-H and a likely weaker microstructure which would further lead to lower compressive strength.

Calcium Carbonate on the other hand is typically forms through the carbonation of $Ca(OH)_2$ when it reacts with atmospheric CO_2. Small amounts of $CaCO_3$ can help fill pores and improve surface hardness. In fact, excessive carbonation may reduce the efficiency of hydration by consuming $Ca(OH)_2$ before it can form C-S-H. Among the samples, EAF_R3_90% had the highest $CaCO_3$ content at 50.0%. According to EDX, this mix also had low calcium (14.35%) and silicon (6.74%) which shows that most of the available calcium

may have carbonated rather than contributing to hydration. This resulted in a weaker and more porous microstructure.

In contrast, EAF_R1_60% and R1_75% had recorded moderate $CaCO_3$ contents of 21.0% and 20.8% respectively. These values when being considered together with their relatively high $Ca(OH)_2$ levels shows a healthy balance between hydration and limited carbonation which could contributing to stronger compressive performance. The control mix contained 26.0% $CaCO_3$ and 13.0% $Ca(OH)_2$. The relatively low $Ca(OH)_2$ content shows that some calcium may have carbonated instead of contributing to further hydration. This could have limited strength development.

Overall, the formation of $Ca(OH)_2$ and $CaCO_3$ is directly influenced by the elemental calcium and silicon available in the mix. When both elements are present in balanced quantities, $Ca(OH)_2$ is more effectively utilized in forming strength-contributing hydration products. This condition is as shown in EAF_R1_75% which had a favorable combination of $Ca(OH)_2$ (21.8%) and $CaCO_3$ (20.8%). In contrast, mixes like R2_90% and R3_90% samples which had either excessive $Ca(OH)_2$ or high $CaCO_3$ combined with low silica shows poor calcium utilization which could resulting in less efficient hydration and weaker mechanical performance.

In conclusion, the XRD findings confirm that the presence and balance of Calcium Hydroxide and Calcium Carbonate are critical indicators of hydration effectiveness and mechanical quality in slag-modified concrete. High $Ca(OH)_2$ levels paired with adequate Si content could promote beneficial hydration reactions while unreacted $Ca(OH)_2$ or excessive $CaCO_3$ which usually under conditions of low silicon can hinder strength performance. Effect of the amount of SiO_2 should also not to be ignored as it also plays a role during the formation of C-S-H gel in hydration process. These results when integrated with EDX elemental data could further highlight the importance of maintaining a well-balanced Ca and Si content to optimize compressive strength especially at higher slag replacement levels.

4.5 Scanning Electron Microscopy (SEM) Test

In this study, the SEM test is being utilized to determine the microstructure and surface characteristics of the samples. The mechanism of this test is by utilizing a focused electron beam to generate images with high resolution. In this study, the sample of Normal Concrete which is also known as “Control” and sample of concrete with specific replacement ratio of EAF slags are being analyzed using this test to determine the crystalline structure present on the sample. By analyzing on the images from SEM, some illustrations of the chemical compound or components could be found such as C-S-H gel, Calcium Hydroxide (Portlandite) and Ettringite. These compounds or components are influencing in contributing to strength development of concrete. Although influence of Ettringite which develop from Aluminum is not as significant as C-S-H gel and Calcium Hydroxide in strength development but its existence in the image could provide some insights however it is not the main concern of this study. These SEM images could further validate and strengthen what had been determined in XRD test by illustrating the chemical compounds or component. This could link the findings which obtained in this part to achieve one of the objective which is to study the elemental and chemical compound composition which affect the compressive strength of concrete with EAF slag replacing fine aggregate at ratio of 60%, 75% and 90%.

For the samples which are being analysed under this test is the normal concrete sample and concrete sample of R1 60%_75%_90%, R2 60%_75%_ 90% and R3 60%_75%_90%. The magnification being used for these samples is being ranged from 1500 X to 3000 X based on the ones which could generate image with best resolution. The SEM images are being shown on the following Figure 4.4 to Figure 4.8. Circles on the figures are use to assist on identification of the surface morphology in the samples. Each of the circles represents different crystalline phases available on the surface of sample where red colour is Ettringite, yellow colour is Portlandite and blue colour is C-S-H gel.

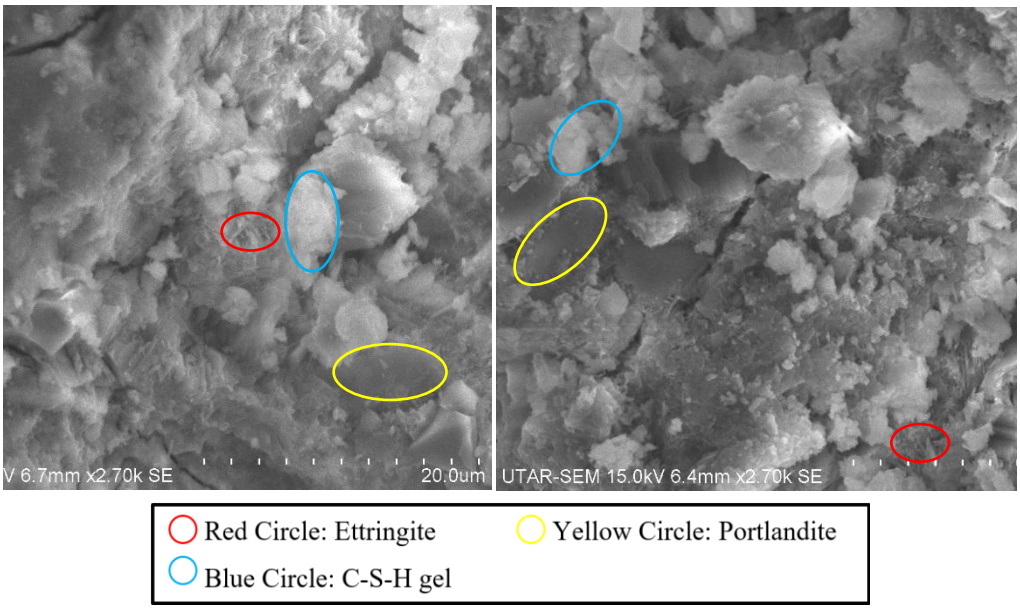

Figure 4.4: SEM of R1 60% (Left). SEM of R1 75% (Right).

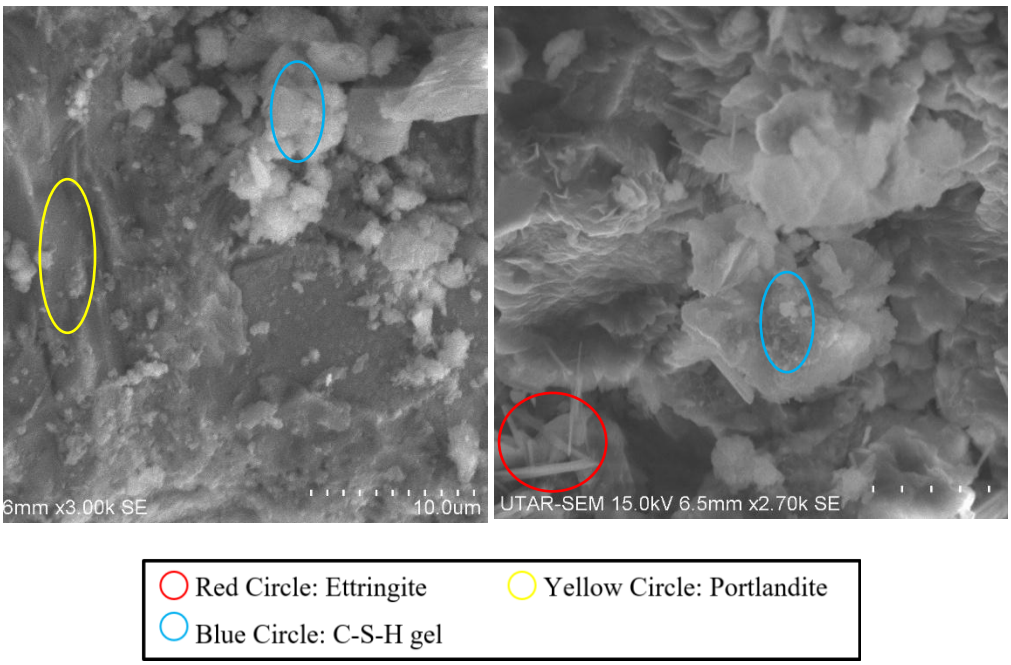

Figure 4.5: SEM of R1 90% (Left). SEM of R2 60% (Right).

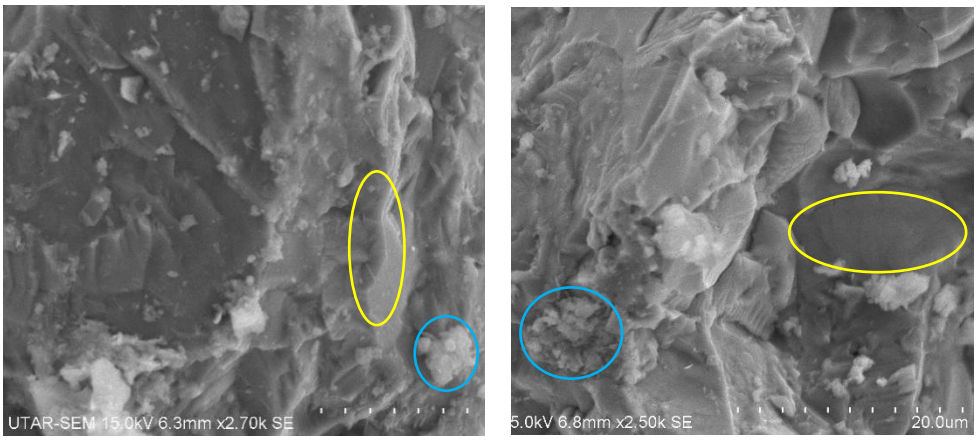

Figure 4.6: SEM of R2 75% (Left). SEM of R2 90% (Right).

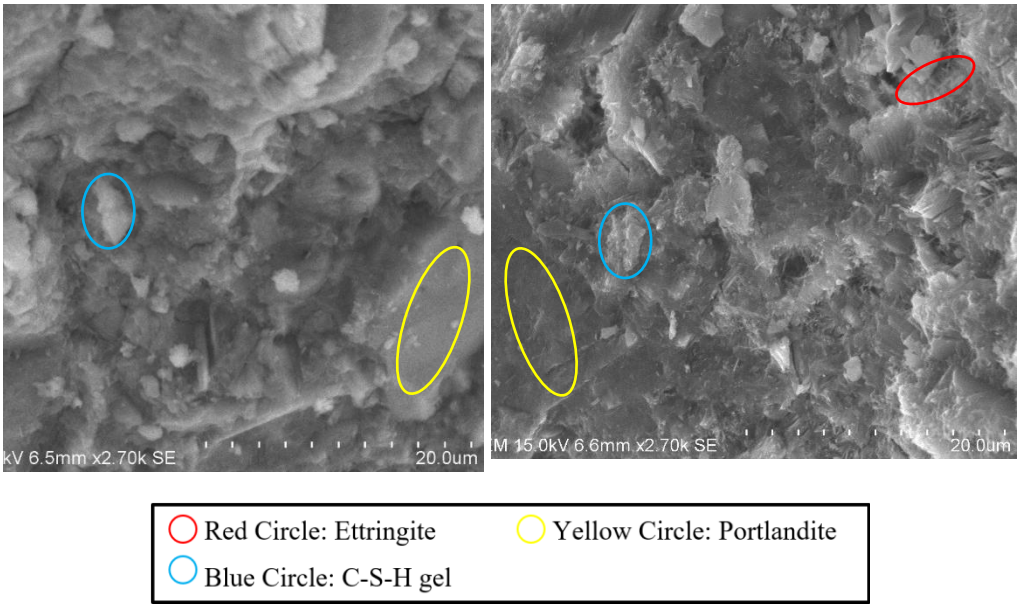

Figure 4.7: SEM of R3 60% (Left). SEM of R3 75% (Right).

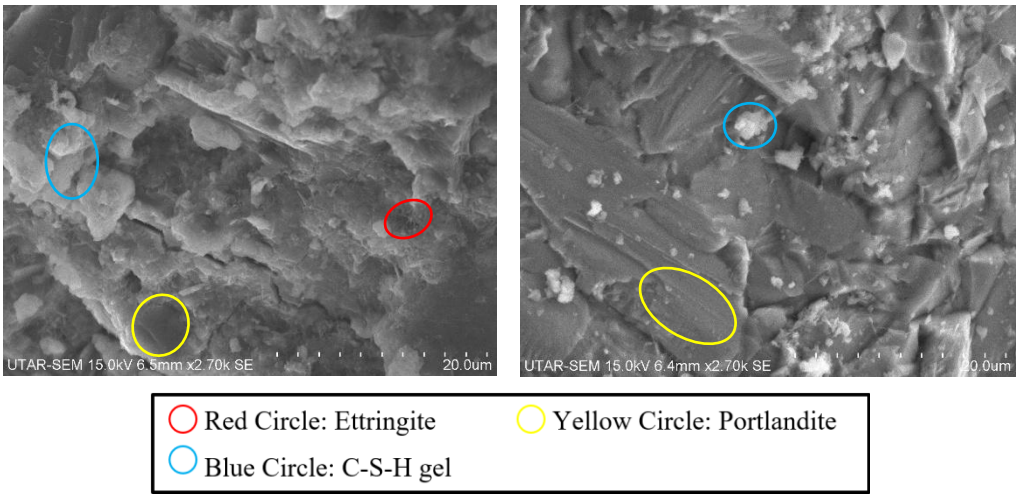

Figure 4.8: SEM of R3 90% (Left). SEM of Control (Right).

4.6 Compression Strength Test

In this study, the test for compression strength of the concrete with EAF slags had been carried out. This strength is one of the component which is important in the mechanical properties of concrete. This test had been done on both normal concrete and concrete with a specified quantity of replacement ratio of EAF slags. The results obtained for this test is being shown in following Table 4.4.

Table 4.4: Compressive Strength of Concrete with EAF Slag under Various Particle Sizes and Replacement Ratio (In Terms of Average).

Compressive Strength in Average (MPa)				
Replacement Ratio of EAF Slag (%)	**Range of Particle Size**			
	Control	**R1**	**R2**	**R3**
0	25.29	0.00	0.00	0.00
60	0.00	51.00	49.00	45.64
75	0.00	52.43	45.92	44.09
90	0.00	54.75	45.93	44.91

Based on the results that obtained and being shown in the above Table 4.4, compressive strength of concrete with EAF slags is between 44 MPa to 55 MPa while the concrete without any replacement of EAF slags (Normal Concrete) achieve the compressive strength of 25 MPa. The trend of the changes

in the compressive strength obtained can be observed better by the bar chart which is shown in Figure 4.9 below.

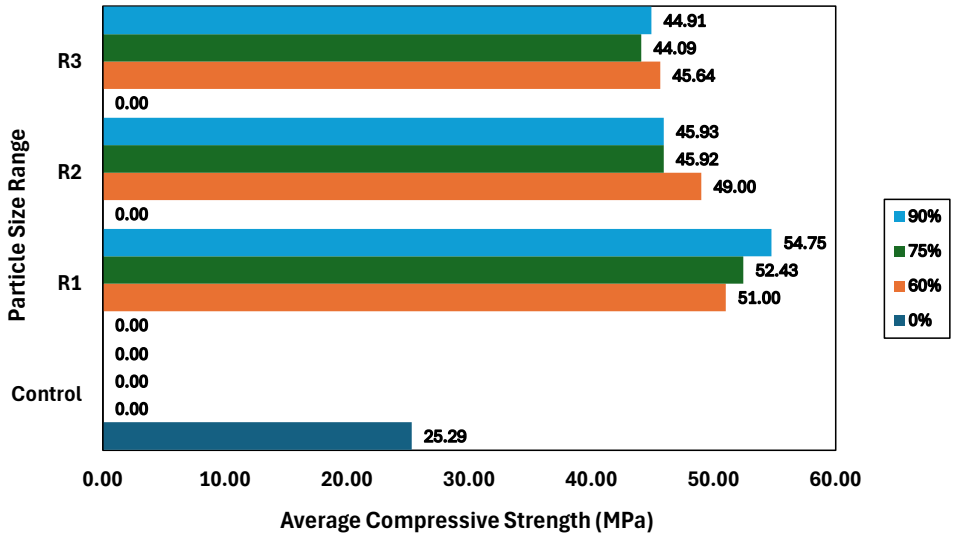

Figure 4.9: Compression Strength of Normal Concrete and Concrete with EAF Slags under Various Particle Size and Replacement Ratio (In Terms of Average).

Based on the values shown in both Table 4.4 and Figure 4.9 above, there are 10 categories in total while each of the categories have 3 cubes. These results are the average value obtained from the test on cubes. This can also be referred to the Table 4.1 above which in total have 30 cubes.

Among the data shown, when the particle size range is being kept as constant variables such as under R2 and observing the trend of changing in increasing replacement ratio, the higher the replacement ratio, the lower the compressive strength is obtained from the test. This relationship is applied to particle size range of R2 (2.36mm to 4.75mm) and R3 (4.75mm to 6.3mm). For R2, the compressive strength recorded for 60%, 75% and 90% are 49.00 MPa, 45.92 MPa and 45.93 MPa respectively while for R3 the compressive strength recorded for 60%, 75% and 90% are 45.64 MPa, 44.09 MPa and 44.91 MPa respectively. The results show that for increasing replacement ratio of 60% to 90%, the compressive strength drops from 49 MPa to 45 MPa for R2 and 45 MPa to 44 MPa for R3. This is due to as the replacement ratio increases, there are more EAF slag replaces sand as fine aggregate in the concrete in terms of

quantity. As EAF slag exhibits more porous properties than natural aggregates, this causes a higher amount of water penetration. Water is an important substance for hydration which is deeply contributed to the compressive strength. Therefore, a higher replacement ratio of EAF slag which means a higher amount of slags are used and this cause water porousity happens more frequently and produce a concrete with lower compressive strength (González-Ortega *et al.*, 2019). However, the result is opposite under R1 particle size range (0.8mm to 2.36mm). In this range, the higher the replacement ratio, the higher compressive strength is obtained as result. For R1, the compressive strength recorded for 60%, 75% and 90% are 51.00 MPa, 52.43 MPa and 54.75 MPa respectively. This is related to the particle size range of EAF slags being used in this condition. As EAF slags is being used as replacement for fine aggregate in concrete, the particle size of sand which is 0.063mm to 2mm (Lees, 2022) could have more effective contact with EAF slags under R1 range. The particle sizes of these 2 materials are more closer to each other and the voids between them could be reduced efficiently. As mentioned that EAF slag particles have the properties of rougher surface texture compared to sand, this could improve the mechanical interlock between the aggregate and the cement paste which could strengthen the interfacial transition zone and improving overall compressive strength (Rondi *et al.*, 2016).

For another condition, where replacement ratio of EAF slag is being kept as a constant variable such as under 60% replacement ratio and observing the changes of result in increasing particle size range, the relation found from the result is the larger particle size range of EAF slags, the lower compressive strength recorded for the concrete. For 60% replacement ratio, the compressive strength for R1, R2 and R3 are 51.00 MPa, 49.00 MPa and 45.64 MPa respectively. For 75% replacement ratio, the compressive strength for R1, R2 and R3 are 52.43 MPa, 45.92 MPa and 44.09 MPa respectively. For 90% replacement ratio, the compressive strength for R1, R2 and R3 are 54.75 MPa, 45.93 MPa and 44.91 MPa respectively. This result could also be justified by referring to the facts as mentioned in R1 range of the previous paragraph. Without regarding to the replacement ratios of 60%, 75% and 90%, as long as the particle size of EAF slags used exceeds 2mm, this could causes the potential of creating voids between the particles as the larger particle size of slags will

create larger voids and requires more particles in concrete to fill up otherwise these voids could reduce the compressive strength. This situation may had happen under this condition (Rondi *et al.*, 2016).

As normal concrete which plays the role as control had also been tested, this study also compares the compressive strength of this concrete with the other concretes with EAF slags. Based on the results stated in Table 4.4 and Figure 4.9, compressive strength of normal concrete is 25 MPa which is lower than those concretes with EAF slags which are in the range of 44 MPa to 55 MPa. This results also tally with previous studies. The previous study done had shown that EAF slag replacement in fine aggregate of concrete could result in production of high-strength concrete compared to conventional mixes. In his study, including 20%, 40%, 60% and 100% EAF slag fine aggregate respectively the 28 days compressive strength was improved by 7.31%, 13.24%, 6.64% and 4.82% respectively (Ozturk *et al.*, 2018).

The compressive strength test results shows that all concrete samples with EAF slag replacement no matter what replacement ratio or particle size range had achieved higher compressive strength than the control mix. This consistent improvement can be attributed to optimized microstructural characteristics as shown through both EDX for elemental composition and XRD for chemical compound composition analysis.

From the EDX test, samples with slag replacement generally shows more balanced and synergistic proportions of Calcium (Ca) and Silicon (Si) which are the two key elements responsible for the formation of Calcium Silicate Hydrate (C-S-H) which is the principal compound contributing to strength in cementitious systems. Although the control sample had a high calcium content (49.85%), it had only 13.83% Si which is similar to several slag-replaced samples such as R1_75% for 8.26%, R1_90% for 8.14%, R3_75% for 8.65%. This shows that although there is abundant Calcium in the control mix, the limited Silica availability may have restricted the full development of C-S-H which causes a less optimized microstructure.

However, slag-modified mixes such as EAF_R1_75%, R1_90% and R2_60% showed not only moderate to high levels of Calcium (21.98%–36.36%) but also adequate Silicon content that likely supported more efficient and continued hydration reactions. This elemental collaboration provided a stronger

foundation for the internal structure which could further contributing to improved compressive strength.

The XRD analysis enhance these findings by showing favorable quantities of hydration-related compounds. In particular, slag-replaced mixes shows controlled levels of $Ca(OH)_2$ which indicating active hydration while also maintaining significantly lower $CaCO_3$ contents compared to the control. For example, the control mix had 26.0% of $CaCO_3$ showing significant carbonation of $Ca(OH)_2$ which not only reduces reactive calcium but can also introduce porosity and long-term durability concerns due to higher amount of $CaCO_3$ may alter the alkalinity environment which could affect the stability of C-S-H gel. In comparison, many slag mixes such as R1_90% (0%), R2_60% (2.0%) and R2_75% (2.0%) had showed minimal $CaCO_3$ formation which showing better preservation of Calcium for hydration and less involvement to carbonation.

Slag replaced samples often had higher SiO_2 content than the control (30.0%). R1_90% contained 60.5% SiO_2 and R2_60% recorded 90.9% showing a richer source of reactive silica which could further support the continued development of C-S-H over time. These mixes which are rich in SiO_2 are more probable to form a denser and more refined microstructure which could enhance overall strength and durability.

Although not the main focus of the study, the particle size characteristics of EAF slag which are being rough and angular may have improved the mechanical interlock with cement paste, enhancing the Interfacial Transition Zone (ITZ) and improving the overall bonding within the matrix. This physical benefit combined with the favorable chemical environment had contributed to the strength improvements which could be observed in slag-replaced samples.

In summary, the improved compressive strength observed in slag-containing mixes is supported by microstructural evidence from both EDX and XRD tests. The images produced in SEM test could further validate the existence of compound such as Calcium Hydroxide and Calcium Carbonate. The slag replacements provided a more optimal balance of calcium and silicon, supported better hydration efficiency and reduced carbonation losses which could resulting in a denser and stronger cementitious matrix than that of the control concrete. These findings confirm that EAF slag when incorporated at

optimised replacement levels can enhance the structural performance of concrete beyond conventional formulations. However, the effect of particle size range of EAF slag on the improvement of compressive strength should also not to be ignored. The findings here which is improved compressive strength had been observed in slag-containing mixes compare with the one of normal concrete could link the findings here to the study objective of to compare the compressive strength between EAF slag concrete and conventional concrete.

Other than that, as replacement ratio of EAF slags in concrete and particle size range of EAF slags used are the 2 variables in this study, an analysis can be carry out to determine the effect of these 2 variables on the compression strength of concrete. This analysis can be carry out by taking the average value of the replacement ratios of EAF slags in concrete and particle size range of EAF slags used respectively. The results under this analysis are being shown in the following Table 4.5 and Figure 4.10.

Table 4.5: Compression Strength of Various Types of Concrete (In Terms of Average).

Different Types of Concrete	**Compressive Strength in Average (MPa)**
R1	52.73
R2	46.95
R3	44.55
60%	48.21
75%	47.48
90%	48.53

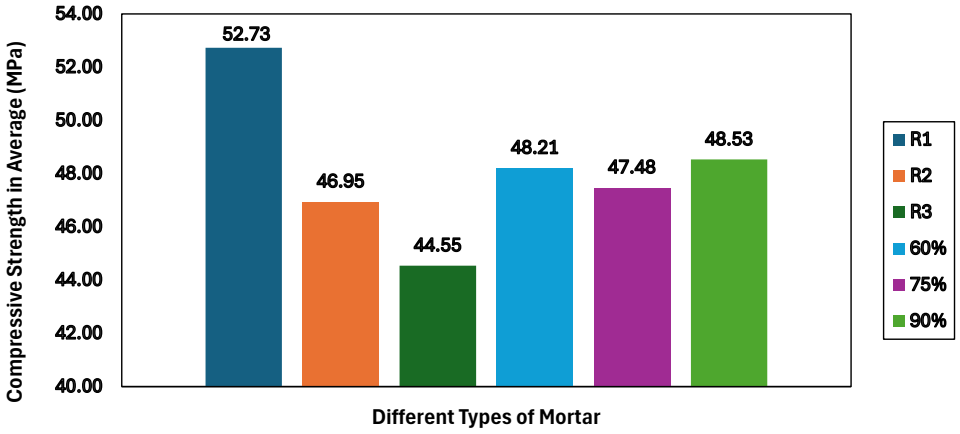

Figure 4.10: Compression Strength of Various Types of Concrete (In Terms of Average).

Based on the results as shown in above Table 4.5 and Figure 4.10, R1 type of concrete had recorded for the highest compression strength with 52.73 MPa while 90% type of concrete had recorded for the second highest compression strength with 48.53 MPa. This result shows that among these 2 variables, particle size range of EAF slags used is the more influencing factor that could affect the compressive strength of concrete. However, this result could only apply for particle size range under R1. As mentioned earlier in the previous paragraph above, the particle size of EAF slag under this range which is 0.8mm to 2.36mm can form a better contact with each other as the sizes is quite similar. EAF slag had also been tested to have favorable frictional characteristics. The morphology which had been found are subrounded to subangular shapes, some very irregularly shaped platy particles were also observed and extremely rough surface texture (Yildirim and Prezzi, 2011). A smaller size of EAF slag particle have larger surface area compare to larger size ones and the favourable frictional characteristics could further enhance the interlocking between particles in concrete. This leads to a higher compressive strength obtained for concrete with EAF slag replacement under this particle size range.

4.7 Thermogravimetric Analysis (TGA) Test

In this section, TGA test is being used in this investigation to determine the changes in mass of the concrete sample. This test is being carried out under controlled heating conditions in order to assess the thermal stability of the concrete samples. Certain conditions are set for the thermal analysis to ensure the reliability for this assessment of the concrete samples' thermal characteristics. To find out potential mass changes during the heating process, the thermal characteristics of concrete samples are studied with a specific temperature range. The mass change is typically due to the decomposition of components inside the concrete sample. This test could provide the information of Weight Loss (WL) which is the mass change of concrete sample. From the analysis of EDX, XRD and SEM tests, several compounds or components such as Calcium Hydroxide, Calcium Carbonates, C-S-H gel (mainly formed by Calcium and Silicon element) and Ettringite had been detected for their existence and this could be implied on the mass change here as the mass change at certain increment of temperature is due to the decomposition of components. These could provide some insights on how the microstructural properties of elemental and compound composition affects the thermal stability of of sample.

In the following Figure 4.11, this figure shows the graphs for results of TGA test. This result is plotted based on the changes of weight for the concrete samples over the temperature. For Table 4.6 below, this shows the summary of TGA results for the samples. In Table 4.6, “TR” represents Temperature Range while “WL” represents for Weight Loss.

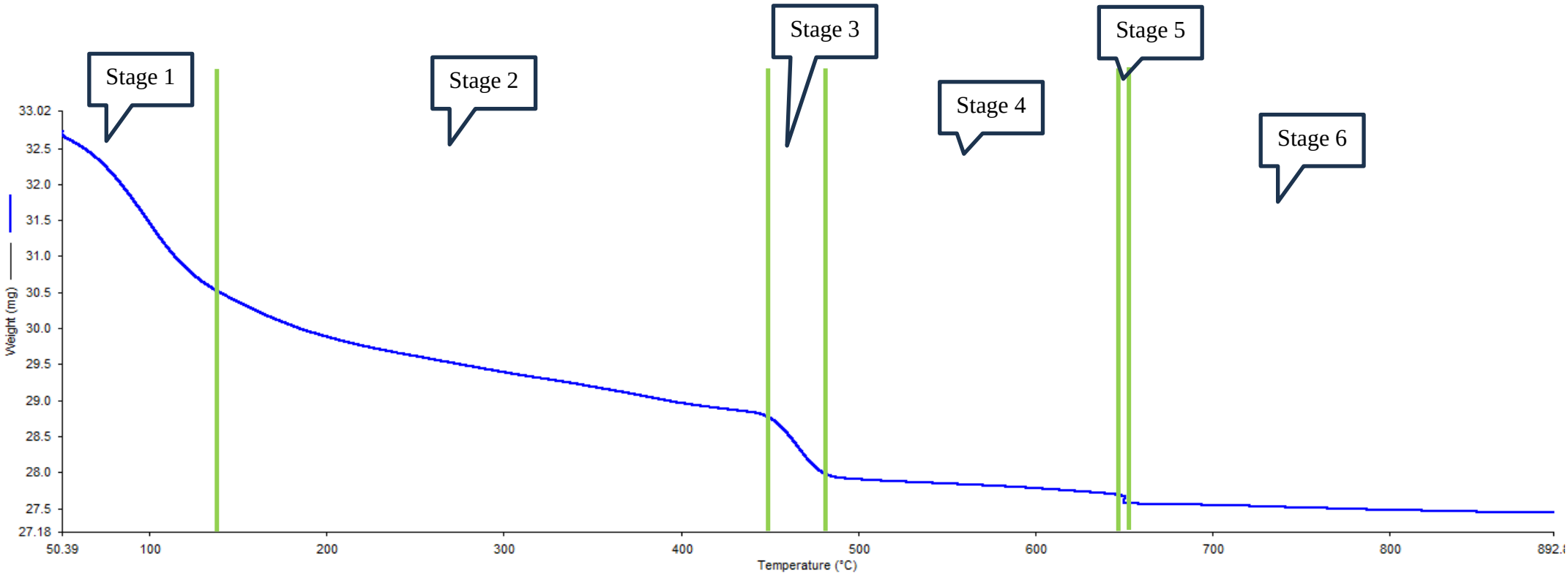

Figure 4.11: TGA Results for the Concrete Samples with EAF Slag under condition R1_EAF_60%.

Table 4.6: Summarized Results of EAF Concrete Samples for TGA Test.

Concrete Samples (EAF)	Stage 1		Stage 2		Stage 3		Stage 4		Stage 5		Stage 6	
	TR (°C)	WL (%)	TR (°C)	WL (%)	TR (°C)	WL (%)	TR (°C)	WL (%)	TR (°C)	WL (%)	TR (°C)	WL (%)
R1_60%	0-140	6.12	140-455	5.81	455-484	2.75	484-660	0.31	660-657	0.33	>657	0.92
R1_75%	0-130	6.20	130-446	5.90	446-460	2.60	460-640	0.28	640-635	0.30	>635	1.00
R1_90%	0-135	6.30	135-430	6.00	430-452	2.45	452-648	0.25	648-643	0.28	>643	1.05
R2_60%	0-143	6.15	143-437	5.85	437-458	2.70	458-652	0.30	652-647	0.32	>647	0.95
R2_75%	0-137	6.35	137-436	6.10	436-455	2.40	455-643	0.24	643-638	0.26	>638	1.10
R2_90%	0-142	6.45	142-450	6.20	450-475	2.20	475-655	0.22	655-650	0.24	>650	1.20
R3_60%	0-140	6.10	140-452	5.80	452-474	2.65	474-650	0.29	650-645	0.31	>645	0.93
R3_75%	0-138	6.25	138-440	6.05	440-468	2.35	468-646	0.23	646-640	0.25	>640	1.12
R3_90%	0-135	6.50	135-435	6.25	435-457	2.15	457-654	0.20	654-650	0.22	>650	1.25

Notes: ‘TR’ represents Temperature Ranges and ‘WL’ represents Weight Loss Percentages

Based on the graph of TGA test in Figure 4.11 above, the concrete sample of EAF_R1_60% is being heated up from 0°C to 892°C. In Stage 1 which is under the temperature range of 0°C to 140°C, the sample had experienced quick changes in weight. In this initial stage, the weight loss that is experienced by the concrete samples is mainly due to the evaporation of free or loosely bound water in the pores which can be found in concrete. This water loss is consider as equivalent for an initial decrease in weight. The weight reduction here which is 6.12% shows there is a relatively high moisture content in the concrete which is normal for concrete materials as this is only the early heating stages (Shoukry *et al.*, 2011).

During this Stage 2 where the temperature range is from 140°C to 455°C, the weight loss can be due to the dehydration of chemically bound water which is those produced from hydration products such as Calcium Silicate Hydrate (C-S-H) and Calcium Aluminate Hydrate (C-A-H). These hydrates are important for concrete strength and their dehydration could causes crucial changes in the concrete microstructure. Partial of Calcium Silicate Hydrate (C-S-H) also starts to degrade at the later part of this temperature range as it start to degrade partially above 400°C. The decreasing trend of Weight Loss is more gradually compares to Stage 1 and this may due to the thermal stability of C-S-H gel as it can maintain thermal stability until 200 to 300°C. C-S-H gel which mainly formed by Calcium and Silicon could improves thermal resistance at moderate temperatures for high amounts of Ca and Si which suggest a well-formed C-S-H network. A 5.81% weight loss recorded during this stage could shows the presence of these hydration products (I. Janotka and Mojumdar, 2005).

For Stage 3 where the samples is being heat up from 455°C to 484°C, the concrete samples had carried out some chemical changes. Calcium Hydroxide ($Ca(OH)_2$) which is a primary hydration product in cementitious matrix starts to degrades partially around 450°C which is near to the initial temperature of this stage. This decomposition causes calcium oxide (CaO) to form and releases water vapor. This causes weight loss to happen. At the same time, this decomposition also shows that the calcium hydroxide content which affects concrete's durability and structural integrity is being affected (Mikhail, Brunauer and Copeland, 1966). Higher $Ca(OH)_2$ content could reduces thermal

stability at elevated temperatures. A higher content of $Ca(OH)_2$ can lead to more degradation and causes larger scale of microcracking, porosity increase and loss of strength.

Stage 4 is where the sample is being heat up from 484°C to 660°C. This heating up causes the further decomposition of Calcium Carbonate ($CaCO_3$) from the concrete's matrix. The loss of Carbon Dioxide (CO_2) due to Calcium Carbonate decomposite causes weight loss here. The quantity of weight loss here can be difference based on the carbonate presence which also affecting the concrete's mechanical properties after heating. It also causes expansion and internal pressure which have the possibility to cause cracking and thermal instability. The presence of Calcium Carbonate here can also act as an indicator of carbonation levels in concrete which could affect the durability (Li *et al.*, 2017).

Next, this stage is Stage 5 where the sample is being heated up but the temperature drops from 660°C to 657°C. In narrow stage of weight changing, this slightly overlap represents the rapid thermal transformations in concrete's silicate structure. This typically involving Calcium Silicates and other minerals present in the EAF slag. Although variations here is only very small but is a valuable observations as this shows the transitions in the microstructure. Changes which happens at this point deeply affect the high-temperature durability and structural integrity of the concrete material (Naus and Graves, 2006).

Lastly, the Stage 6 is heating up the sample from 657°C to 892°C. This also indicates the ending of heating process for the sample in this TGA Test. This final stage also shows the thermal decomposition and structural deterioration of the sample. Within this highest temperature range, fire-durable minerals and other complex chemical components starts to break down. This leads to a very significant weight loss and critical degradation of concrete's mechanical properties and structural integrity. The weight losses here shows the thermal limit where concrete with EAF slag replacement may experiencing failures or loses its critical function. By understanding the phenomenon happen in this stage, this could also provide guidance for assessing the fire resistance and long-term durability of concrete structures especially those which are

containing high volumes of slags as certain material's replacement (Ivanka Netinger Grubeša, Marija Jelčić Rukavina and Mladenović, 2016).

In a nutshell, the concrete samples with EAF slag had been determined for their thermal stability by using the TGA test. Throughout the Table 4.6, several different temperature ranges and weight loss percentage can be observed. However, in order to determine a certain weight loss percentage is considered thermally stable or not, this still need to be consider based on several factors such as composition of slag, required properties and usage.

4.8 Optimal Replacement Ratio of EAF Slag

In the context of this study, the concept of optimal replacement ratio refers to the ratio of EAF slag used to replace natural fine aggregate of concrete that produces the most favorable combination of mechanical performance and microstructural quality. While broader definitions of "optimal" may consider factors such as durability, workability or cost-effectiveness, this study scopes optimality primarily based on compressive strength results which supported by microstructural evaluations using EDX and XRD analysis. Therefore, the optimal replacement ratio in this context is the one that delivers the highest compressive strength while also demonstrating balanced elemental composition and compound formation that enhance durable and well-structured concrete.

Among all tested samples, EAF_R1_90% was identified as the optimal mix which achieving the highest compressive strength of 54.75 MPa. This is more than double of the control mix which recorded only 25.29 MPa. This significant improvement highlights the higher load-bearing capability of the concrete mix incorporating 90% EAF slag within the R1 particle size range (0.8–2.36 mm). The strength gain is further supported by elemental composition from EDX analysis which shows that EAF_R1_90% contains 36.36% calcium and 8.14% silicon. Both are critical for the formation of Calcium Silicate Hydrate (C-S-H) which is the primary compound responsible for strength development in concrete. Although the control sample had a higher calcium content of 49.85%, its relatively low silicon content (13.83%) may have limited the full formation of C-S-H and this further reducing its strength potential.

In addition to EDX, the XRD analysis confirms the microstructural advantage of EAF_R1_90%. The sample shows a high Silicon Dioxide (SiO_2)

content of 60.5% which is a strong indicator of abundant reactive silica in the system. The Calcium Hydroxide ($Ca(OH)_2$) level was moderately high at 29.1% showing the active hydration was taking place while the absence of Calcium Carbonate ($CaCO_3$) shows minimal carbonation which means that most of the available calcium remained in a reactive or beneficial state which is being hydrated. The low free CaO content which is 1.16% shows that excess calcium was effectively integrated into hydration products instead of remaining unreacted which could contribute to the overall microstructural cohesion and durability of the mix.

Although particle size was not the primary focus of the study, the use of finer EAF slag particles in the R1 range has the favourable to enhance the hydration process due to greater surface area and better particle packing. This could have improved the density and strength of the Interfacial Transition Zone (ITZ) between aggregate and cement paste which contributing to the higher mechanical performance observed in EAF_R1_90%.

In summary, EAF_R1_90% can be considered the optimal replacement ratio in this study as it shows the optimized mechanical performance with microstructural indicators that support hydration efficiency and strength development. Its balanced Calcium and Silicon, minimal carbonation and high compressive strength further enhance its effectiveness as a high-performing and sustainable alternative compare to conventional fine aggregate such as natural sand in concrete.

4.9 Summary

This chapter shows the results from several tests done on concrete samples made with EAF slag. The tests include Compression Strength Test, SEM Test, EDX Test, XRD Test and TGA Test. These tests help to have better understanding on the strength, chemical compounds, elements and heat resistance of concrete mixed with EAF slag.

The Compression Strength Test found that concrete with EAF slag has higher strength which is in the range of 44 to 55 MPa compared to normal concrete which is 25 MPa. The highest compressive strength is recorded when 90% replacement ratio is used especially with smaller EAF slag particles (R1).

Energy-Dispersive X-ray Spectroscopy (EDX) Test is used to study about the elements inside the concrete. Calcium (Ca) and Silicon (Si) are important for development mechanical properties which is the compressive strength in this study. Samples with higher calcium content especially when paired with sufficient silica shows stronger hydration potential and better internal bonding which contributing to improved compressive strength. Mixes with low calcium showed reduced strength due to inefficient hydration and weaker microstructural development.

X-ray Diffraction (XRD) Test is used to show what chemical compounds are available in the sample. The analysis showed that the presence and balance of Calcium Hydroxide ($Ca(OH)_2$) and Calcium Carbonate ($CaCO_3$) can significantly affect the compressive strength of EAF slag concrete. Moderate and Moderate-to-high $Ca(OH)_2$ levels when matched with sufficient silica can supported effective hydration. In contrast, excessive $Ca(OH)_2$ or high $CaCO_3$ levels especially in mixes with low Si, indicated poor calcium utilization and were associated with weaker microstructures and lower strength. These findings highlight the importance of maintaining a balanced chemical composition to optimize hydration efficiency and mechanical performance.

Scanning Electron Microscopy (SEM) Test study at the different surface of the concrete. Images generated had showed some crystals such as the Ettringite which labelled in red circle, Portlandite which labelled in yellow circle and C-S-H gel which labelled in blue circle. Several points of cracks and rough surfaces are observed from the images.

The Compression Strength Test found that concrete with EAF slag has the optimal compressive strength which is in the range of 44 to 55 MPa compared to normal concrete which is 25 MPa. The optimal compressive strength is recorded when 90% replacement ratio is used.

Thermogravimetric Analysis (TGA) Test helps to measure weight change of sample when heated. Microstructural properties such as the amount of C-S-H gel, $Ca(OH)_2$ and $CaCO_3$ could affect the thermal stability by microcracks, expansion and internal pressure etc. Majority of water content in the sample lost below 455°C and majority of chemical substance breakdown after 450°C. Concrete with EAF slag maintain stable until about 660°C. After

that, damage started to happen. The temperature range for decomposition is from 0°C to approximately 900°C.

CHAPTER 5

CONCLUSION AND RECOMMENDATIONS

5.1 Conclusion

This study focus on determining the mechanical and microstructural properties of concrete using Electric Arc Furnace (EAF) slag as a partial replacement for fine aggregate at several ratios of 60%, 75% and 90%. The EAF slags used is categorized into three particle size ranges which are R1 (0.80–2.36 mm), R2 (2.36–4.75 mm) and R3 (4.75–6.30 mm). This study aims to determine the mechanical properties which is compressive strength through evaluating the microstructural properties of elemental and chemical compound composition of concrete with EAF slag replacement.

The first objective of this study is to compare the compressive strength between EAF slag concrete and conventional concrete. Results obtained for compressive strength shows that concrete with partial replacement of EAF slag is higher than compressive strength of normal concrete. Normal concrete had recorded for a compressive strength of only 25 MPa. The highest strength was observed in the R1_EAF_90% sample which achieved 54. 75MPa. This improvement is due to the finer particle size of the R1 group which could provide better particle packing, reduced voids and improved bonding between the EAF slag and the cement paste. Therefore, 90% replacement with the using of R1 particles was found to be the relatively more effective combination for maximizing compressive strength.

The second objective of this study is to determine the optimal replacement ratio of EAF slag which could provide optimal compressive strength. Throughout this study, the optimal replacement ratio being concluded is 90%. This could be further supported by the elemental analysis in Energy-Dispersive X-ray Spectroscopy (EDX) test and chemical compound analysis in X-ray Diffraction (XRD) test. Elements which affect the compressive strength development are Calcium and Silicon. High Calcium content (36.36%) and Silicon content (8.14%) had been obtained under this replacement ratio. For the Calcium Hydroxide ($Ca(OH)_2$) and Calcium Carbonate ($CaCO_3$) content, sample with 90% replacement ratio had moderate-to-high amount of Calcium

Hydroxide (29.10%) but 0% of Calcium Carbonate content. This indicates that this high amount of Calcium content have sufficient Silicon supply which could leads to a strong hydration potential and minimal carbonation which could support a denser microstructure and higher compressive strength. Low to No content of Calcium Carbonate is detected further reduce the risk of reducing the efficiency of hydration by consuming $Ca(OH)_2$ before it can form C-S-H which could produce a weaker and more porous microstructure. Images from Scanning Electron Microscopy (SEM) could further validates the existence of these 2 compounds in the sample. Compressive Strength which is the optimal is also recorded on 90% replacement.

The third objective of the study is to study the elemental and chemical compound composition which affect the compressive strength of concrete with EAF slag replacing fine aggregate at ratio of 60%, 75% and 90%. Throughout the study and referring to research which had done earlier, it can be concluded that Calcium (Ca) and Silicon (Si) are the elements which affect the compressive strength development. Samples with higher calcium content especially when paired with sufficient silica shows stronger hydration potential and better internal bonding which contribute to improved compressive strength. For chemical compound composition, it can be concluded that the Calcium Hydroxide ($Ca(OH)_2$) and Calcium Carbonate ($CaCO_3$) are the compounds which affect the compressive strength development. Moderate and Moderate-to-high $Ca(OH)_2$ levels when matched with sufficient silica can support effective hydration. High $CaCO_3$ levels especially in mixes with low Si indicates poor calcium utilization and associated with weaker microstructures and lower strength.

These findings shows the importance of optimizing the replacement ratio when partially replacing fine aggregate of concrete with EAF slag. The optimized replacement ratio should also used with the optimal particle size ranges. Influence of optimal particle size should not be ignored to ensure maximization of benefits obtained. This replacement ratio could also be a sustainable solution for improving both mechanical performance and environmental impact in construction materials at the same time.

5.2 Recommendations for future work

While this study shows the results of utilizing the replacement of Electric Arc Furnace (EAF) slag as fine aggregate in concrete, there are still some of the areas which are valuable to further study beyond the findings. Firstly, future research could study on the other mechanical properties of EAF slag concrete such as flexural strength, tensile strength, modulus of elasticity and impact resistance. This could help to obtain a more complete and detail understanding of the structural performance of concrete sample with EAF slag replacement under different loading conditions.

In this study, only the thermal stability had been studied. Future work could also focus on studying the long-term durability which including resistance to chloride penetration, sulphate attack, carbonation depth and freeze-thaw cycles. These evaluations are important for assessing the concrete's performance in extreme environmental conditions.

Another important direction would be to broaden the sample diversity. This study used only EAF slag from a single source in Penang. However, chemical composition of EAF slag can have variation by regional or production process. Therefore, using the slags from different steel plants across Malaysia or countries over the world could help to increase the accuracy and reliability of the results obtained.

Lastly, developing and testing the common concrete elements such as beams, panels or pavement slabs could provide more insight on assessing real-life constructability, workability and curing behavior. These studies could help to provide more information on linking results obtained from laboratory investigations to industrial applications. This could pave the way for EAF slag concrete to be applied more widely in construction practices nowadays which also urging for sustainability.

REFERENCE

Aldea, C.-M., Young, F., Wang, K. and Shah, S.P. (2000). Effects of curing conditions on properties of concrete using slag replacement. *Cement and Concrete Research*, 30(3), pp.465–472. doi:https://doi.org/10.1016/s0008-8846(00)00200-3.

Allen, D.J. and Brent, G.F. (2010). Sequestering CO2 by Mineral Carbonation: Stability against Acid Rain Exposure. *Environmental Science & Technology*, 44(7), pp.2735–2739. doi:https://doi.org/10.1021/es903212j.

Anon, (2024). *Hydrocarbon Traps*. [online] Available at: https://www.geologyin.com/2014/12/hydrocarbon-traps.html.

Araner (2024). *Thermocline Layer | ARANER District Cooling*. [online] Araner.com. Available at: https://www.araner.com/blog/thermocline-layer#:~:text=In%20stratified%20Thermal%20Energy%20Storage [Accessed 28 Aug. 2024].

Aresta, M. and Dibenedetto, A. (2010). Industrial utilization of carbon dioxide (CO2). *Developments and Innovation in Carbon Dioxide (CO2) Capture and Storage Technology*, pp.377–410. doi:https://doi.org/10.1533/9781845699581.4.377.

Baciocchi, R., Costa, G., Polettini, A. and Pomi, R. (2009). Influence of particle size on the carbonation of stainless steel slag for CO2 storage. *Energy Procedia*, 1(1), pp.4859–4866. doi:https://doi.org/10.1016/j.egypro.2009.02.314.

Baras, A., Li, J., Wen, N., Hussain, Z. and Hitch, M. (2023). Evaluation of Potential Factors Affecting Steel Slag Carbonation. *Processes*, 11(9), pp.2590–2590. doi:https://doi.org/10.3390/pr11092590.

Bimal Raut. (2022). *Thermogravimetric Analysis: Principle, Instrumentation, and Reliable Application - Chemistry Notes*. [online] Available at: https://chemistnotes.com/analytical_chemistry/thermogravimetric-analysis-principle-instrumentation-and-reliable-application/.

Brewer, P.G., Peltzer, E.T., Friederich, G., Aya, I. and Yamane, K. (2000). Experiments on the ocean sequestration of fossil fuel CO2: pH measurements and hydrate formation. *Marine Chemistry*, 72(2-4), pp.83–93. doi:https://doi.org/10.1016/s0304-4203(00)00074-8.

Bruker (2024). *What is EDS? | Energy Dispersive X-Ray Spectroscopy*. [online] www.bruker.com. Available at: https://www.bruker.com/en/landingpages/bna/technology/what-is-eds.html.

Chang, J., Xiong, C., Zhang, Y. and Wang, D. (2019). Foaming characteristics and microstructure of aerated steel slag block prepared by accelerated carbonation. *Construction and Building Materials*, 209, pp.222–233. doi:https://doi.org/10.1016/j.conbuildmat.2019.03.077.

CO_2 Sequestration by Mineral Carbonation: A Review. (2018). *Issue 3*, 20(3), pp.497–503. doi:https://doi.org/10.30955/gnj.002597.

Davidson, J., Freund, P., Smith, A. (2001). Putting carbon back into the ground. IEA Greenhouse Gas R&D Programme

de Coninck, H. and Benson, S.M. (2014). Carbon Dioxide Capture and Storage: Issues and Prospects. *Annual Review of Environment and Resources*, 39(1), pp.243–270. doi:https://doi.org/10.1146/annurev-environ-032112-095222.

DiGiovanni, C., Hisseine, O.A. and Adedapo Noah Awolayo (2024). Carbon dioxide sequestration through steel slag carbonation: Review of mechanisms, process parameters, and cleaner upcycling pathways. *Journal of CO2 utilization*, 81, pp.102736–102736. doi:https://doi.org/10.1016/j.jcou.2024.102736.

drawellanalytical (2023). *What is XRD(X-ray Diffraction) - Advantages, Types and How it Works - Drawell*. [online] Available at: https://www.drawellanalytical.com/what-is-xrdx-ray-diffraction-advantages-types-and-how-it-works/.

Fathy, S., Liping, G., Ma, R., Chunping, G. and Wei, S. (2018). Comparison of Hydration Properties of Cement-Carbon Steel Slag and Cement-Stainless Steel Slag Blended Binder. *Advances in Materials Science and Engineering*, 2018(1). doi:https://doi.org/10.1155/2018/1851367.

FERNANDEZBERTOS, M., SIMONS, S., HILLS, C. and CAREY, P. (2004). A review of accelerated carbonation technology in the treatment of cement-based materials and sequestration of CO2. *Journal of Hazardous Materials*, [online] 112(3), pp.193–205. doi:https://doi.org/10.1016/j.jhazmat.2004.04.019.

Fisher, L.V. and Barron, A.R. (2021). Suitability of Steel Making Slag as a Construction Material Resource. *Recent Progress in Materials*, 03(03), pp.1–1. doi:https://doi.org/10.21926/rpm.2103028.

G, O.W., Freund, P., Smith, A., comps and Davison, J. (2002). *Ocean storage of CO{sub 2}. 2nd rev. ed.* [online] Osti.gov. Available at: https://www.osti.gov/etdeweb/biblio/20310116 [Accessed 28 Aug. 2024].

Gentzis, T. (2000). Subsurface sequestration of carbon dioxide — an overview from an Alberta (Canada) perspective. *International Journal of Coal Geology*, 43(1-4), pp.287–305. doi:https://doi.org/10.1016/s0166-5162(99)00064-6.

Ghacham, A.B., Pasquier, L.-C., Cecchi, E., Blais, J.-F. and Mercier, G. (2016). CO2 sequestration by mineral carbonation of steel slags under ambient temperature: parameters influence, and optimization. *Environmental Science and Pollution Research*, 23(17), pp.17635–17646. doi:https://doi.org/10.1007/s11356-016-6926-4.

Gibbins, J. and Chalmers, H. (2008). Carbon capture and storage. *Energy Policy*, [online] 36(12), pp.4317–4322. doi:https://doi.org/10.1016/j.enpol.2008.09.058.

GOFF, F. and LACKNER, K.S. (1998). Carbon Dioxide Sequestering Using Ultramaf ic Rocks. *Environmental Geosciences*, 5(3), pp.89–102. doi:https://doi.org/10.1046/j.1526-0984.1998.08014.x.

González-Ortega, M.A., Cavalaro, S.H.P., Rodríguez de Sensale, G. and Aguado, A. (2019). Durability of concrete with electric arc furnace slag aggregate. *Construction and Building Materials*, 217, pp.543–556. doi:https://doi.org/10.1016/j.conbuildmat.2019.05.082.

Han, D.-R., Namkung, H., Lee, H.-M., Huh, D.-G. and Kim, H.-T. (2015). CO 2 sequestration by aqueous mineral carbonation of limestone in a supercritical reactor. *Journal of industrial and engineering chemistry/Journal of Industrial and Engineering Chemistry - Korean Society of Industrial and Engineering Chemistry*, 21, pp.792–796. doi:https://doi.org/10.1016/j.jiec.2014.04.014.

Herzog, H. (2024). *OCEAN SEQUESTRATION OF CO 2 -AN OVERVIEW*. [online] Available at: https://web.mit.edu/energylab/www/pubs/overview.PDF.

Herzog, H.J., 1998, August. Ocean sequestration of CO2: an overview. In *Proceedings of the AWMA's Second International Specialty Conference, Oct 13-15, 1998, Washington, DC*.

Holappa, L. (2020). A General Vision for Reduction of Energy Consumption and CO2 Emissions from the Steel Industry. *Metals*, 10(9), p.1117. doi:https://doi.org/10.3390/met10091117.

Hosseini, S., Soltani, S.M., Fennell, P.S., Choong, T.S.Y. and Aroua, M.K. (2016). Production and applications of electric-arc-furnace slag as solid waste in environmental technologies: a review. *Environmental Technology Reviews*, 5(1), pp.1–11. doi:https://doi.org/10.1080/21622515.2016.1147615.

Huang, X., Zhang, J. and Zhang, L. (2024). Accelerated carbonation of steel slag: A review of methods, mechanisms and influencing factors. *Construction & building materials*, 411, pp.134603–134603. doi:https://doi.org/10.1016/j.conbuildmat.2023.134603.

Hui Xing Zhang, Anand Chokkalingam, Subramaniam, P.V., Joseph, S., Takeuchi, S., Ming Deng Wei, Al-Enizi, A.M., Jang, H.-G., Kim, J.-H., Seo, G., Kenichi Komura, Yoshihiro Sugi and Ajayan Vinu (2016). The isopropylation of biphenyl over transition metal substituted aluminophosphates: MAPO-5 (M: Co and Ni). *Journal of Molecular Catalysis A Chemical*, 412, pp.117–124. doi:https://doi.org/10.1016/j.molcata.2015.11.006.

Huijgen, W.J.J., Witkamp, G.-J. and Comans, R.N.J. (2006). Mechanisms of aqueous wollastonite carbonation as a possible CO2 sequestration process. *Chemical Engineering Science*, 61(13), pp.4242–4251. doi:https://doi.org/10.1016/j.ces.2006.01.048.

I. Janotka and Mojumdar, S.C. (2005). Thermal analysis at the evaluation of concrete damage by high temperatures. *Journal of Thermal Analysis and Calorimetry*, 81(1), pp.197–203. doi:https://doi.org/10.1007/s10973-005-0767-6.

Ivanka Netinger Grubeša, Marija Jelčić Rukavina and Mladenović, A. (2016). Impact of High Temperature on Residual Properties of Concrete with Steel Slag Aggregate. *Journal of Materials in Civil Engineering*, 28(6). doi:https://doi.org/10.1061/(asce)mt.1943-5533.0001515.

Jägemann, C., Fürsch, M., Hagspiel, S. and Nagl, S. (2013). Decarbonizing Europe's power sector by 2050 — Analyzing the economic implications of alternative decarbonization pathways. *Energy Economics*, 40, pp.622–636. doi:https://doi.org/10.1016/j.eneco.2013.08.019.

Ko, M.-S., Chen, Y.-L. and Jiang, J.-H. (2015). Accelerated carbonation of basic oxygen furnace slag and the effects on its mechanical properties. *Construction and Building Materials*, 98, pp.286–293. doi:https://doi.org/10.1016/j.conbuildmat.2015.08.051.

Kumi Oyamada, Tsukidate, M., Watanabe, K., Takahashi, T., Tsuneo Isoo and Toshinobu Terawaki (2008). A field test of porous carbonated blocks used as artificial reef in seaweed beds of Ecklonia cava. *Journal of Applied Phycology*, 20(5), pp.863–868. doi:https://doi.org/10.1007/s10811-008-9332-6.

Lackner, K.S., Wendt, C.H., Butt, D.P., Joyce, E.L. and Sharp, D.H. (1995). Carbon dioxide disposal in carbonate minerals. *Energy*, 20(11), pp.1153–1170. doi:https://doi.org/10.1016/0360-5442(95)00071-n.

Ledley, T.S., Sundquist, E.T., Schwartz, S.E., Hall, D.K., Fellows, J.D. and Killeen, T.L. (1999). Climate change and greenhouse gases. *Eos, Transactions American Geophysical Union*, [online] 80(39), pp.453–458. doi:https://doi.org/10.1029/99eo00325.

Lees, A. (2022). *What is Particle Size Distribution in Soils?* [online] Tensarinternational.com. Available at: https://www.tensarinternational.com/resources/articles/what-is-particle-size-distribution-in-soils [Accessed 10 Nov. 2024].

Lekakh, S.N., Rawlins, C.H., Robertson, D.G.C., Richards, V.L. and Peaslee, K.D. (2008). Kinetics of Aqueous Leaching and Carbonization of Steelmaking Slag. *Metallurgical and Materials Transactions B*, 39(1), pp.125–134. doi:https://doi.org/10.1007/s11663-007-9112-8.

Li, M., Lu, Y., Liu, Y., Chu, J., Zhang, T. and Wang, W. (2024). Influence of the Steel Slag Particle Size on the Mechanical Properties and Microstructure of Concrete. *Sustainability*, 16(5), pp.2083–2083. doi:https://doi.org/10.3390/su16052083.

Li, Q., Song, R., Liu, X., Liu, G. and Sun, Y. (2016a). Monitoring of Carbon Dioxide Geological Utilization and Storage in China: A Review. pp.331–358. doi:https://doi.org/10.1002/9781118938652.ch22.

Li, Q., Wei, Y.-N. and Chen, Z.-A. (2015). Water-CCUS nexus: challenges and opportunities of China's coal chemical industry. *Clean Technologies and Environmental Policy*, 18(3), pp.775–786. doi:https://doi.org/10.1007/s10098-015-1049-z.

Li, X., Lv, Y., Ma, B., Wang, W. and Jian, S. (2017). Decomposition kinetic characteristics of calcium carbonate containing organic acids by TGA. *Arabian Journal of Chemistry*, 10, pp.S2534–S2538. doi:https://doi.org/10.1016/j.arabjc.2013.09.026.

Luo, Z., Wang, Y., Yang, G., Ye, J., Zhang, W., Liu, Z. and Mu, Y. (2021). Effect of curing temperature on carbonation behavior of steel slag compacts. 291, pp.123369–123369. doi:https://doi.org/10.1016/j.conbuildmat.2021.123369.

Mahinpey, N., Asghari, K. and Mirjafari, P. (2011). Biological sequestration of carbon dioxide in geological formations. *Chemical Engineering Research and Design*, 89(9), pp.1873–1878. doi:https://doi.org/10.1016/j.cherd.2010.10.016.

Mahoutian, M. and Shao, Y. (2016). Production of cement-free construction blocks from industry wastes. *Journal of Cleaner Production*, 137, pp.1339–1346. doi:https://doi.org/10.1016/j.jclepro.2016.08.012.

Mahoutian, M., Ghouleh, Z. and Shao, Y. (2014). Carbon dioxide activated ladle slag binder. *Construction and Building Materials*, 66, pp.214–221. doi:https://doi.org/10.1016/j.conbuildmat.2014.05.063.

Manso, J.M., Polanco, J.A., Losañez, M. and González, J.J. (2006). Durability of concrete made with EAF slag as aggregate. *Cement and Concrete Composites*, 28(6), pp.528–534. doi:https://doi.org/10.1016/j.cemconcomp.2006.02.008.

Maroto-Valer, M.M. (Ed.), 2010. Developments and Innovation in Carbon Dioxide (CO_2) Capture and Storage Technology. Woodhead Publising Limited, Cambridge.

Maslehuddin, M., Sharif, A.M., Shameem, M., Ibrahim, M. and Barry, M.S. (2003). Comparison of properties of steel slag and crushed limestone aggregate concretes. *Construction and Building Materials*, 17(2), pp.105–112. doi:https://doi.org/10.1016/s0950-0618(02)00095-8.

Meima, J.A., van der Weijden, R.D., Eighmy, T.Taylor. and Comans, R.N.J. (2002). Carbonation processes in municipal solid waste incinerator bottom ash and their effect on the leaching of copper and molybdenum. *Applied Geochemistry*, [online] 17(12), pp.1503–1513. doi:https://doi.org/10.1016/s0883-2927(02)00015-x.

Mignone, B.K., Sarmiento, J.L., Slater, R.D. and Gnanadesikan, A. (2004). Sensitivity of sequestration efficiency to mixing processes in the global ocean. *Energy*, 29(9-10), pp.1467–1478. doi:https://doi.org/10.1016/j.energy.2004.03.080.

Mikhail, R.Sh., Brunauer, S. and Copeland, L.E. (1966). Kinetics of the thermal decomposition of calcium hydroxide. *Journal of Colloid and Interface Science*, 21(4), pp.394–404. doi:https://doi.org/10.1016/0095-8522(66)90005-5.

Mo, L., Deng, M., Tang, M. and Al-Tabbaa, A. (2014). MgO expansive cement and concrete in China: Past, present and future. *Cement and Concrete Research*, 57, pp.1–12. doi:https://doi.org/10.1016/j.cemconres.2013.12.007.

Mokobi, F. (2020). *Scanning Electron Microscope (SEM)*. [online] Microbe Notes. Available at: https://microbenotes.com/scanning-electron-microscope-sem/.

Naidu, T.S., Sheridan, C.M. and van Dyk, L.D. (2020). Basic oxygen furnace slag: Review of current and potential uses. *Minerals Engineering*, 149, p.106234. doi:https://doi.org/10.1016/j.mineng.2020.106234.

Naus, D.J. and Graves, H. (2006). A Review of the Effects of Elevated Temperature on Concrete Materials and Structures. *Volume 1: Plant Operations, Maintenance and Life Cycle; Component Reliability and Materials Issues; Codes, Standards, Licensing and Regulatory Issues; Fuel Cycle and High Level Waste Management*. doi:https://doi.org/10.1115/icone14-89631.

Neville, A.M. (2011). *Properties of Concrete*. Prentice Hall.

Ngala, V.T. and Page, C.L. (1997). EFFECTS OF CARBONATION ON PORE STRUCTURE AND DIFFUSIONAL PROPERTIES OF HYDRATED CEMENT PASTES. *Cement and Concrete Research*, 27(7), pp.995–1007. doi:https://doi.org/10.1016/s0008-8846(97)00102-6.

Nielsen, P., Boone, M.A., Horckmans, L., Snellings, R. and Quaghebeur, M. (2020). Accelerated carbonation of steel slag monoliths at low CO2 pressure – microstructure and strength development. *Journal of CO2 Utilization*, 36, pp.124–134. doi:https://doi.org/10.1016/j.jcou.2019.10.022.

Oelkers, E.H., Gislason, S.R. and Matter, J. (2008). Mineral Carbonation of CO2. *Elements*, 4(5), pp.333–337. doi:https://doi.org/10.2113/gselements.4.5.333.

Olajire, A.A. (2013). A review of mineral carbonation technology in sequestration of CO2. *Journal of Petroleum Science and Engineering*, [online] 109, pp.364–392. doi:https://doi.org/10.1016/j.petrol.2013.03.013.

Oyamada, K., Okamoto, M. and Iwata, I., 2014. Development of restoration technology for coral reefs using "Marine Block™". *JFE Tech Rep*, *19*, pp.118-125.

Ozaki, M., Junichi Minamiura, Kitajima, Y., Mizokami, S., Takeuchi, K. and Katsunori Hatakenaka (2001). CO 2 ocean sequestration by moving ships. *Journal of marine science and technology*, 6(2), pp.51–58. doi:https://doi.org/10.1007/s773-001-8375-8.

Ozturk, M., Akgol, O., Sevim, U.K., Karaaslan, M., Demirci, M. and Unal, E. (2018). Experimental work on mechanical, electromagnetic and microwave shielding effectiveness properties of mortar containing electric arc furnace slag. *Construction and Building Materials*, 165, pp.58–63. doi:https://doi.org/10.1016/j.conbuildmat.2018.01.031.

Pan, K., Li, H.Q., Wang, C.Y., Bao, W.J., Huang, K.L. and Liao, D.K. (2014). Enhanced Steelmaking Slag Mineral Carbonation in Dilute Alkali Solution. *Advanced Materials Research*, 878, pp.244–253. doi:https://doi.org/10.4028/www.scientific.net/amr.878.244.

Pan, S.-Y., Chung, T.-C., Ho, C.-C., Hou, C.-J., Chen, Y.-H. and Chiang, P.-C. (2017). CO2 Mineralization and Utilization using Steel Slag for Establishing a Waste-to-Resource Supply Chain. *Scientific Reports*, 7(1). doi:https://doi.org/10.1038/s41598-017-17648-9.

Pang, B., 2016. Prepration and Property Investigation of Carbonated Steel Slag Aggregate and Concrete. Master's Thesis, Jinan University, Jinan, China.

Papadakis, V.G. (2000). Effect of supplementary cementing materials on concrete resistance against carbonation and chloride ingress. *Cement and Concrete Research*, 30(2), pp.291–299. doi:https://doi.org/10.1016/s0008-8846(99)00249-5.

Pellegrino, C. and Gaddo, V. (2009). Mechanical and durability characteristics of concrete containing EAF slag as aggregate. *Cement and Concrete Composites*, 31(9), pp.663–671. doi:https://doi.org/10.1016/j.cemconcomp.2009.05.006.

Pires, J.C.M., Martins, F.G., Alvim-Ferraz, M.C.M. and Simões, M. (2011). Recent developments on carbon capture and storage: An overview. *Chemical Engineering Research and Design*, 89(9), pp.1446–1460. doi:https://doi.org/10.1016/j.cherd.2011.01.028.

Polettini, A., Pomi, R. and Stramazzo, A. (2016). Carbon sequestration through accelerated carbonation of BOF slag: Influence of particle size characteristics. *Chemical Engineering Journal*, 298, pp.26–35. doi:https://doi.org/10.1016/j.cej.2016.04.015.

Power, I.M., Dipple, G.M. and Southam, G. (2009). Bioleaching of Ultramafic Tailings by Acidithiobacillus spp. for CO2 Sequestration. *Environmental Science & Technology*, 44(1), pp.456–462. doi:https://doi.org/10.1021/es900986n.

Prigiobbe, V., Polettini, A. and Baciocchi, R. (2009). Gas–solid carbonation kinetics of Air Pollution Control residues for CO2 storage. *Chemical Engineering Journal*, 148(2-3), pp.270–278. doi:https://doi.org/10.1016/j.cej.2008.08.031.

Qasrawi, H., Shalabi, F. and Asi, I. (2009). Use of low CaO unprocessed steel slag in concrete as fine aggregate. *Construction and Building Materials*, 23(2), pp.1118–1125. doi:https://doi.org/10.1016/j.conbuildmat.2008.06.003.

Rađenović, A., Malina, J. and Sofilić, T. (2013). Characterization of Ladle Furnace Slag from Carbon Steel Production as a Potential Adsorbent. *Advances in Materials Science and Engineering*, 2013, pp.1–6. doi:https://doi.org/10.1155/2013/198240.

Ragipani, R., Bhattacharya, S. and Suresh, A.K. (2021). A review on steel slag valorisation via mineral carbonation. *Reaction Chemistry & Engineering*. doi:https://doi.org/10.1039/d1re00035g.

Røkke, N.A. and Langørgen, Ø. (2009). Enabling pre-combustion plants—the DECARBit project. *Energy Procedia*, 1(1), pp.1435–1442. doi:https://doi.org/10.1016/j.egypro.2009.01.188.

Rondi, L., Bregoli, G., Sorlini, S., Cominoli, L., Collivignarelli, C. and Plizzari, G. (2016). Concrete with EAF steel slag as aggregate: A comprehensive technical and environmental characterisation. *Composites Part B: Engineering*, 90, pp.195–202. doi:https://doi.org/10.1016/j.compositesb.2015.12.022.

Santos, R.M., Ling, D., Sarvaramini, A., Guo, M., Elsen, J., Larachi, F., Beaudoin, G., Blanpain, B. and Van Gerven, T. (2012). Stabilization of basic oxygen furnace slag by hot-stage carbonation treatment. *Chemical Engineering Journal*, 203, pp.239–250. doi:https://doi.org/10.1016/j.cej.2012.06.155.

Saran, R.K., Kumar, R., Yadav, S. (2017a). Climate change: mitigation strategyby various CO2 sequestration methods. International Journal of Advanced Research in Science, Engineering, 6, 299–308.

SciMed (2023). *A Brief Introduction to SEM (Scanning Electron Microscopy) | SciMed*. [online] SciMed. Available at: https://www.scimed.co.uk/education/sem-scanning-electron-microscopy/.

Shi, C. (2004). Steel Slag—Its Production, Processing, Characteristics, and Cementitious Properties. *Journal of Materials in Civil Engineering*, 16(3), pp.230–236. doi:https://doi.org/10.1061/(asce)0899-1561(2004)16:3(230).

Shi, D., Ye, J., Zhang, W., Si, K., Zhang, M. and Zhang, H., 2021. Synergistic mechanism of alkali-activation and carbonation of carbonated steel slag bricks. *J. Iron Steel Res*, *33*, pp.1127-1133.

Shoukry, S.N., William, G.W., Downie, B. and Riad, M.Y. (2011). Effect of moisture and temperature on the mechanical properties of concrete. *Construction and Building Materials*, 25(2), pp.688–696. doi:https://doi.org/10.1016/j.conbuildmat.2010.07.020.

Shu Yuan Pan, Hsing Lu Liu, Chang, E.E., Kim, H., Yi Hung Chen and Pen Chi Chiang (2016). Multiple model approach to evaluation of accelerated carbonation for steelmaking slag in a slurry reactor. *Chemosphere*, 154, pp.63–71. doi:https://doi.org/10.1016/j.chemosphere.2016.03.093.

Siddique, R. (2014). Utilization of Industrial By-products in Concrete. *Procedia Engineering*, 95, pp.335–347. doi:https://doi.org/10.1016/j.proeng.2014.12.192.

Siddique, R. and Bennacer, R. (2012). Use of iron and steel industry by-product (GGBS) in cement paste and mortar. *Resources, Conservation and Recycling*, [online] 69, pp.29–34. doi:https://doi.org/10.1016/j.resconrec.2012.09.002.

Skaf, M., Manso, J.M., Aragón, Á., Fuente-Alonso, J.A. and Ortega-López, V. (2017). EAF slag in asphalt mixes: A brief review of its possible re-use. *Resources, Conservation and Recycling*, 120, pp.176–185. doi:https://doi.org/10.1016/j.resconrec.2016.12.009.

Skaf, M., Ortega-López, V., Fuente-Alonso, J.A., Santamaría, A. and Manso, J.M. (2016). Ladle furnace slag in asphalt mixes. *Construction and Building Materials*, 122, pp.488–495. doi:https://doi.org/10.1016/j.conbuildmat.2016.06.085.

Skalny, J., Marchand, J. and Odler, I., 2003. *Sulfate attack on concrete* (No. 15832). Taylor & Francis.

Song, Q., Guo, M.-Z., Wang, L. and Ling, T.-C. (2021). Use of steel slag as sustainable construction materials: A review of accelerated carbonation treatment. *Resources, Conservation and Recycling*, [online] 173, p.105740. doi:https://doi.org/10.1016/j.resconrec.2021.105740.

Song, Q., Guo, M.-Z., Wang, L. and Ling, T.-C. (2021). Use of steel slag as sustainable construction materials: A review of accelerated carbonation treatment. *Resources, Conservation and Recycling*, [online] 173, p.105740. doi:https://doi.org/10.1016/j.resconrec.2021.105740.

Song, Q., Guo, M.-Z., Wang, L. and Ling, T.-C. (2021). Use of steel slag as sustainable construction materials: A review of accelerated carbonation treatment. *Resources, Conservation and Recycling*, [online] 173, p.105740. doi:https://doi.org/10.1016/j.resconrec.2021.105740.

Stelios Antiohos and S. Tsimas (2009). *Mechanical and durability characteristics of concrete containing EAF slag as aggregate*. [online] Cement and Concrete Composites. Available at: https://www.academia.edu/30069306/Mechanical_and_durability_characteristics_of_concrete_containing_EAF_slag_as_aggregate [Accessed 20 Apr. 2025].

Substech.com. (2012). *Basic Oxygen Furnace (BOF) [SubsTech]*. [online] Available at: https://www.substech.com/dokuwiki/doku.php?id=basic_oxygen_furnace_bof.

T. Isoo, Takahashi, T., Okamoto, N. and Fukuhara, M. (2000). Development of large steelmaking slag blocks using a new carbonation process. *Advances in Cement Research*, 12(3), pp.97–101. doi:https://doi.org/10.1680/adcr.2000.12.3.97.

Tapia, J.F.D., Lee, J.-Y., Ooi, R.E.H., Foo, D.C.Y. and Tan, R.R. (2018). A review of optimization and decision-making models for the planning ofCO2capture, utilization and storage (CCUS) systems. *Sustainable Production and Consumption*, 13, pp.1–15. doi:https://doi.org/10.1016/j.spc.2017.10.001.

Teir, S., Eloneva, S., Fogelholm, C.-J. and Zevenhoven, R. (2006). Stability of calcium carbonate and magnesium carbonate in rainwater and nitric acid solutions. *Energy Conversion and Management*, 47(18-19), pp.3059–3068. doi:https://doi.org/10.1016/j.enconman.2006.03.021.

thermofisher (2024). *Energy Dispersive X-ray Spectroscopy | EDS Analysis | EDX Analysis - US*. [online] Available at: https://www.thermofisher.com/my/en/home/materials-science/learning-center/eds-analysis.html.

Thiery, M., Villain, G., Dangla, P. and Platret, G. (2007). Investigation of the carbonation front shape on cementitious materials: Effects of the chemical kinetics. *Cement and Concrete Research*, 37(7), pp.1047–1058. doi:https://doi.org/10.1016/j.cemconres.2007.04.002.

Tsakiridis, P.E., Papadimitriou, G.D., Tsivilis, S. and Koroneos, C. (2008). Utilization of steel slag for Portland cement clinker production. *Journal of Hazardous Materials*, [online] 152(2), pp.805–811. doi:https://doi.org/10.1016/j.jhazmat.2007.07.093.

Ukwattage, N.L., Ranjith, P.G. and Li, X. (2017). Steel-making slag for mineral sequestration of carbon dioxide by accelerated carbonation. *Measurement*, 97, pp.15–22. doi:https://doi.org/10.1016/j.measurement.2016.10.057.

von der Assen, N., Voll, P., Peters, M., Bardow, A. (2014). Life cycle assessment of CO_2 capture and utilization; a tutorial review. Chem. Soc. Rev. 43, 7982-7994.

Voormeij, D. and Simandl, G. (2024). Geological, Ocean, and Mineral CO2 Sequestration Options: A Technical Review. *Geoscience Canada*, [online] 31(1), pp.11–22. Available at: https://id.erudit.org/iderudit/geocan31_1art02 [Accessed 28 Aug. 2024].

W.J.J., H. and R.N.J., C. (2003). Carbon dioxide sequestration by mineral carbonation. Literature Review. [online] Available at: https://inis.iaea.org/search/search.aspx?orig_q=RN:34066562.

Wall, T., Liu, Y., Spero, C., Elliott, L., Khare, S., Rathnam, R., Zeenathal, F., Moghtaderi, B., Buhre, B., Sheng, C., Gupta, R., Yamada, T., Makino, K. and Yu, J. (2009). An overview on oxyfuel coal combustion—State of the art research and technology development. *Chemical Engineering Research and Design*, 87(8), pp.1003–1016. doi:https://doi.org/10.1016/j.cherd.2009.02.005.

Wang, L., Sarkar, B., Sonne, C., Ok, Y.S. and Tsang, D.C.W. (2020). Soil and geologic formations as antidotes for CO_2 sequestration?. *Soil Use and Management*, 36(3), pp.355–357. doi:https://doi.org/10.1111/sum.12589.

Wang, X., Chang, Y., Zhu, D., Li, S., Geng, S., Chang, Y., Chen, Y., Mao, M. and Zhang, M. (2021). Integrating Circulating Tumor DNA Features and Plasma Protein Markers to Detected Early Lymphoid Neoplasm. *Blood*, 138(Supplement 1), pp.4489–4489. doi:https://doi.org/10.1182/blood-2021-145683.

Wang, Y., Liu, J., Hu, X., Chang, J., Zhang, T. and Shi, C. (2022). Utilization of accelerated carbonation to enhance the application of steel slag: a review. *Journal of Sustainable Cement-Based Materials*, pp.1–16. doi:https://doi.org/10.1080/21650373.2022.2154287.

Wei, X., Wen, N., Zhang, S., Wang, X., Li, J. and Du, H. (2022). Influence of the key factors on the performance of steel slag-desulphurisation gypsum-based hydration-carbonation materials. *Journal of building engineering*, 45, pp.103591–103591. doi:https://doi.org/10.1016/j.jobe.2021.103591.

Xue, Y., Wu, S., Hou, H., Zha, J., 2006. Experimental investigation of basic oxygen furnace slag used as aggregate in asphalt mixture. J. Hazard. Mater. 138 (2), 261–268. https://doi.org/10.1016/j.jhazmat.2006.02.073.

Yadav, S. and Mehra, A. (2021). A review on ex situ mineral carbonation. *Environmental Science and Pollution Research*, 28(10), pp.12202–12231. doi:https://doi.org/10.1007/s11356-020-12049-4.

Ye, J., Zhang, W., Shi, D., Si, Z. and Chen, X., 2019. Synergistic effect of alkali-activation and carbonation on carbonated steel slag bricks. *J. Chin. Ceram. Soc*, *47*, pp.1582-1592.

Yi, H., Xu, G., Cheng, H., Wang, J., Wan, Y. and Chen, H. (2012). An Overview of Utilization of Steel Slag. *Procedia Environmental Sciences*, [online] 16, pp.791–801. doi:https://doi.org/10.1016/j.proenv.2012.10.108.

Yildirim, I.Z. and Prezzi, M. (2011). Chemical, Mineralogical, and Morphological Properties of Steel Slag. *Advances in Civil Engineering*, 2011, pp.1–13. doi:https://doi.org/10.1155/2011/463638.

Yu, J. and Wang, K. (2011). Study on Characteristics of Steel Slag for CO_2Capture. *Energy & Fuels*, 25(11), pp.5483–5492. doi:https://doi.org/10.1021/ef2004255.

Zhong, X., Li, L., Jiang, Y. and Ling, T.-C. (2021). Elucidating the dominant and interaction effects of temperature, CO2 pressure and carbonation time in carbonating steel slag blocks. *Construction and Building Materials*, 302, p.124158. doi:https://doi.org/10.1016/j.conbuildmat.2021.124158.